

TRACING ORIGIN AND COLLAPSE OF HOLOCENE BENTHIC BASELINE COMMUNITIES IN THE NORTHERN ADRIATIC SEA

IVO GALLMETZER,¹ ALEXANDRA HASELMAIR,¹ ADAM TOMAŠOVÝCH,² ANNA-KATHARINA MAUTNER,¹ SARA-MARIA SCHNEDL,¹ DANIELE CASSIN,³ ROBERTO ZONTA,³ AND MARTIN ZUSCHIN¹
¹University of Vienna, Department of Paleontology, Althanstraße 14, 1090 Vienna, Austria
²Earth Science Institute, Slovak Academy of Sciences, Dúbravská cesta 9, 84005 Bratislava, Slovak Republic
³Consiglio Nazionale delle Ricerche, Istituto di Scienze Marine, Castello 2737/F, 30122 Venice, Italy
email: ivo.gallmetzer@univie.ac.at

ABSTRACT: The shallow northern Adriatic Sea has a long history of anthropogenic impacts that reaches back many centuries. While the effects of eutrophication, overfishing, pollution, and trawling over recent decades have been extensively studied, the major ecological turnovers during the Holocene as a whole remain poorly explored. In this study, we reconstruct ecological baselines defining benthic ecosystem composition prior to major anthropogenic changes at four stations characterized by low sedimentation and millennial-scale time averaging of molluscan assemblages. We discriminate between natural and anthropogenic drivers based on (1) stratigraphic changes in the composition of molluscan communities observed in sediment cores and (2) changes in concentrations of heavy metals, pollutants, and organic enrichment. The four 1.5-m long sediment cores reach back to the Pleistocene–Holocene boundary, allowing for a stratigraphic distinction of the major sea-level phases of the Holocene. During the transgressive phase and maximum flooding, sea-level and establishment of the modern circulation pattern determined the development of benthic communities in shallow-water, vegetated habitats with epifaunal biostromes and, in deeper waters, with bryozoan meadows. After sea-level stabilization, the composition of these baseline communities remained relatively uniform and started to change markedly only with the intensification of human impacts in the late highstand, leading to a dominance of infauna and a decline of epifauna at all sites. This profound ecological change reduced species richness, increased the abundance of infaunal suspension feeders, and led to a decline of grazers and deposit feeders. We suggest that modern soft-bottom benthic communities in the northern Adriatic Sea today do not show the high geographic heterogeneity in composition characteristic of benthos prior to anthropogenic influences.

INTRODUCTION

The northern Adriatic Sea is a young ecosystem that originated at the onset of the Holocene, approximately 11,000 years ago, when rising sea level inundated the vast alluvial plains that had been exposed since the Würmian glaciation (Brambati 1992; Amorosi et al. 2008). In contrast to most other shallow coastal seas worldwide, it was affected by a dense human colonization of shores and hinterlands from early on in mankind's history (Turney and Brown 2007). The anthropogenic alteration of Adriatic ecosystems probably reached an initial peak as early as the time of the Roman Empire, with local exhaustion of fish stocks and increased river sediment loads due to deforestation-induced erosion (Kaligarić et al. 2006; Lotze et al. 2011). Human pressure rose again in the Middle Ages due to population growth and the expansion of coastal settlements (Lotze et al. 2006). During the last 200 years, the human impact on continental shelves has increased exponentially with the many repercussions of industrialization and a globalized economy: eutrophication, deoxygenation, pollution, coastal development, and an enormous fishing pressure at global scales including the Northern Adriatic Sea (Justić 1991; Jackson et al. 2001; Airoldi and Beck 2007; Occhipinti-Ambrogi 2007; Roberts 2007; Zillén et al. 2008; Rabalais et al. 2010; Coll et al. 2012; Tomašových and Kidwell 2017).

Several paleoecological studies have demonstrated effects of overfishing, eutrophication, hypoxia, and pollution on ecosystem composition in the northern Adriatic over the past few centuries based on historical and

sediment core data (Barnawidjaja et al. 1995; Sangiorgi and Donders 2004; Ferretti et al. 2013; Kowalewski et al. 2015; Vidović et al. 2016; Gallmetzer et al. 2017; Tomašových et al. 2017, 2019). However, quantitative analyses of benthic assemblages in sediment cores capturing time intervals preceding the past 500 years are rare, and the major ecological turnovers in the northern Adriatic during the entire Holocene remain poorly explored, especially in the north-eastern part (Fiorini and Vaiani 2001; Scarponi and Kowalewski 2007; Rossi and Vaiani 2008; Lotze et al. 2011; Coll and Lotze 2016).

In view of the long-lasting human influence and in the absence of long-term stratigraphic records, it is difficult to reconstruct ecological baselines defining the ecosystem prior to major anthropogenic changes, and to disentangle the effects of long-term ecological drivers such as the post-glacial sea-level rise or climatic oscillations from human interference (Kidwell 2015; Martinelli et al. 2017; Casebolt and Kowalewski 2018).

Here, based on multiple marine sediment cores that capture the entire Holocene in the northern Adriatic Sea, we investigate down-core shifts within the molluscan community and use them as indicators for changes in the marine environment (Anderson et al. 1998; Poirier et al. 2009; Cramer et al. 2015; Gallmetzer et al. 2017). Sediment analyses for heavy metals, organic pollutants, and nutrient concentrations (proxies for human impacts) supplement the findings from the molluscan death assemblages and help in discriminating between natural and anthropogenic drivers of observed community changes. Geochronological data are based on two methods: (1)

^{210}Pb of sediment, which provides constraints on apparent sedimentation rates over the past ~ 120 years, with rate estimates being sensitive to bioturbation (Peng et al. 1979), and (2) Radiocarbon-calibrated amino acid racemization (AAR) dating of mollusk shells from several layers evenly distributed along the sediment cores. These methods allow for a temporal classification of community shifts and also for an assessment of the degree of mixing between layers, one of the major challenges in inferences based on subfossil assemblages (Scarponi et al. 2013; Tomašových et al. 2014; Kosnik et al. 2015; Ritter et al. 2017; Kowalewski et al. 2018).

The four sediment cores used for this study (each 1.5 m long) are from widely separated sampling stations and are thus representative of a broad range of low-sedimentation settings in the northern Adriatic. They not only help draw a comprehensive picture of the ecological history of the whole basin, but also illustrate the heterogeneity of its soft-bottom habitats.

The long time-span embraced in the relatively short sediment columns of 1.5 m has repercussions for the temporal resolution of the ecological history preserved in the cores. In addition to low sediment accumulation rate, bioturbation complicates the detectability of shorter-term shifts by disrupting original stratification and mixing shells of considerably different age (Kosnik et al. 2007; Tomašových et al. 2017). This time-averaging, however, also implies that the environmental and ecosystem trends detected in the cores represent a strong and conservative signal, one that survived in spite of mixing (Tomašových and Kidwell 2010).

The geochronology and molluscan abundance data of the cores from the Brijuni Islands, Croatia, and from the two stations off the coast of Slovenia (stations Piran 1 and 2) were described by Schnedl et al. (2018), Mautner et al. (2018), and Tomašových et al. (2019). Here, we describe age distributions from a fourth station off the Venice lagoon, Italy, and comprehensively analyze stratigraphic (within stations) and geographic variation (among stations) in molluscan composition.

We use molluscan communities as surrogates of macrobenthic soft-bottom assemblages (Olsford and Somerfield 2000; Kidwell 2002; Albano et al. 2016; Tyler and Kowalewski 2017), and trace long-term shifts in their composition from the beginning of the marine transgression ($\sim 11,500$ years BP at 40 m depth and $\sim 9,000$ years BP at 20 m depth; Colantoni et al. 1979; Storms et al. 2008; Schnedl et al. 2018) through the maximum ingressions ($\sim 7,000$ – $5,500$ years ago; Trincardi et al. 2011; Amorosi et al. 2017) to the highstand communities established $\sim 5,500$ years ago. Controlling for centennial-scale climatic oscillations, such shelly assemblages can be considered as baseline communities, a term used here to denote the range of compositional states that characterized benthic communities at the onset of the first major human impacts in recent centuries. At the same time, our approach reveals the turning points in Holocene community developments marked by anthropogenic pressures of various kinds, and helps quantify the amount of species turnover or habitat degradation in relation to former ecosystem conditions. As such, our work also provides clues for possible restoration or conservation efforts by identifying ecological reference conditions.

MATERIAL AND METHODS

Study Area and Sampling Stations

The shallow northern Adriatic Sea (average depth 35 m) is delimited from the mid-Adriatic basin by a 50-m isobath extending approximately from the southern tip of the Istrian Peninsula to Ancona on the Italian coast. It is one of the few modern epicontinental seas comparable to typical Paleozoic and Mesozoic shelf environments (McKinney 2007). The inflow of the Po River and other smaller rivers along the western margin leads to high sediment and nutrient input, making this area one of the most productive in the generally oligotrophic Mediterranean (Zavatarelli et al. 1998). Because of the prevailing counterclockwise currents, nutrients and sediments are asymmetrically distributed along a west-east gradient, with

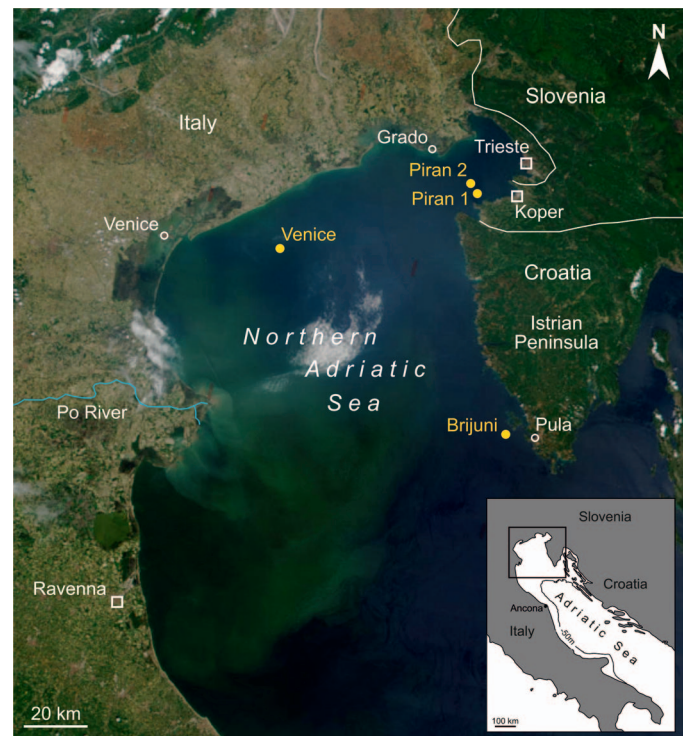


FIG. 1.—The four sampling stations “Venice”, “Brijuni”, “Piran 1” and “Piran 2” in the northern Adriatic Sea. The satellite image shows a major westward increase in the influence of the Po River responsible for the sediment plume that is transported southward. The eastern margins of the northern Adriatic Sea are characterized by lower water turbidity (Image credit: Jacques Desclotres, MODIS Land Rapid Response Team, NASA/GSFC).

meso- to eutrophic waters in the western and northern part and oligotrophic conditions in the eastern regions (Smoldaka 1986; Zuschin and Stachowitsch 2009). The trophic state fluctuates seasonally due to stable water column stratification in summer and pronounced mixing processes caused by winter storms (Giani et al. 2012). In general, the northern Adriatic seafloor is formed by fine-grained sands on the inner shelf, by silts and clays on the middle shelf, and by relict Pleistocene sands on the outer shelf, with the thickness of the Holocene muds decreasing strongly with distance from the coastline (Frigani et al. 2005). Most terrigenous muds are deposited as a belt along the western coast, where they accumulate at annual rates locally exceeding 1 cm/year (Palinkas and Nittrouer 2007; Tesi et al. 2011; Albano et al. 2017). In contrast, the eastern karst-dominated coast is sediment starved (Colantoni and Mencucci 2010) and the Holocene marine sedimentary cover in the southern Gulf of Trieste also tends to be very thin (Trobec et al. 2018).

The four sampling stations were selected to cover different sediment types and degrees of protection from bottom trawling (Fig. 1). Station “Venice” is located about 18 km south-east of the Venice Lagoon in Italian waters at a depth of 21 m ($45.375233^{\circ}\text{N}$, $12.775783^{\circ}\text{E}$). The sediment is almost pure sand and is covered by large amounts of shell debris interspersed with rhodolites and occasional sessile and vagile epifauna (ascidians, sponges, hermit crabs, scallops) (Fig. 2A). Station “Brijuni” is located within the boundaries of the Brijuni Islands National Park (Croatia), at the southern tip of Veliki Brijuni Island, ~ 400 m from shore, at a water depth of 44 m ($44.885833^{\circ}\text{N}$, $13.747017^{\circ}\text{E}$). The seafloor consists of muddy sand and, at the time of sampling, showed signs of mucilage cover, Lebensspuren, and half-buried shell fragments (Fig. 2B). This location has been protected from fishing activity since 1983 when the

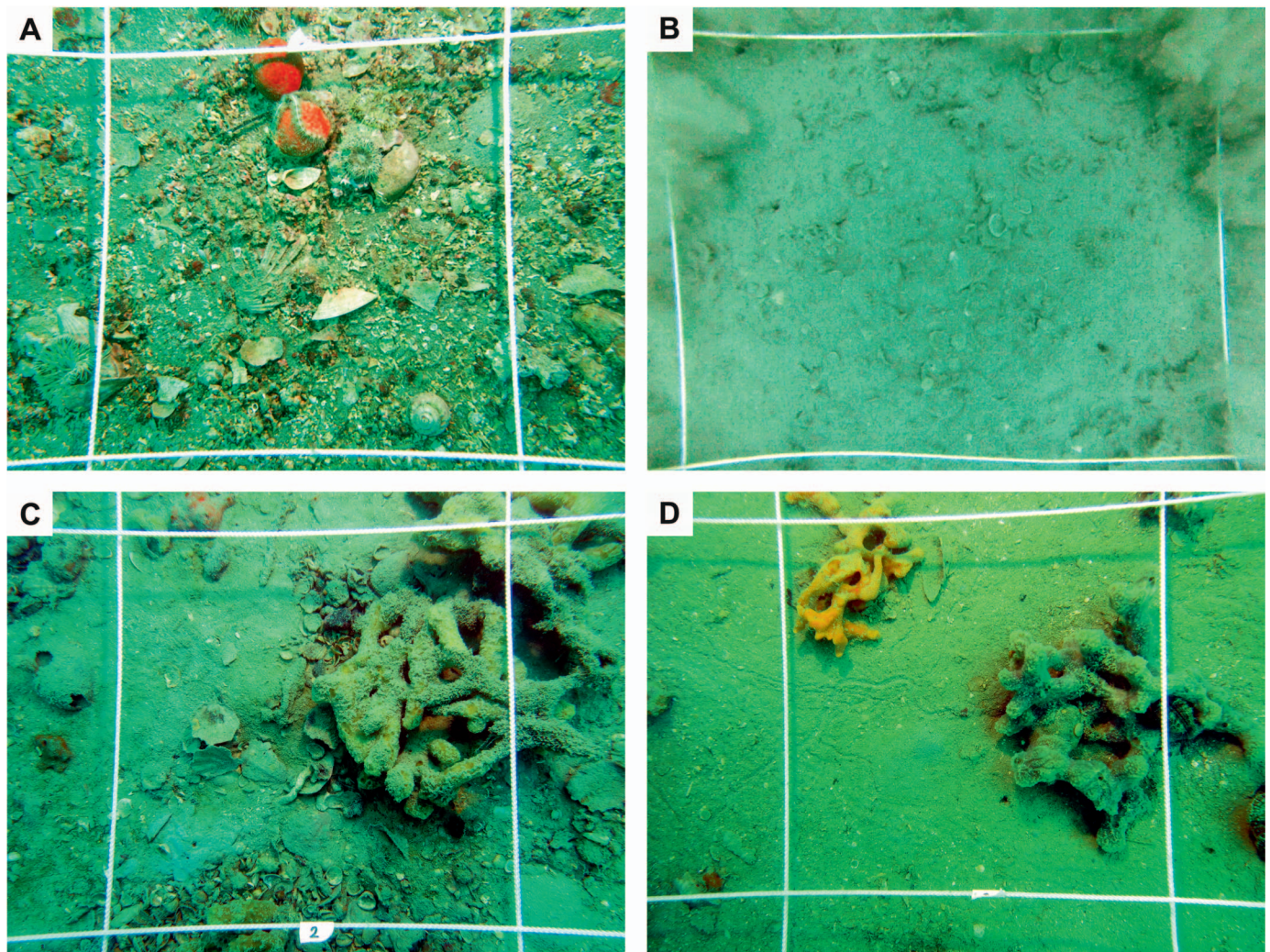


FIG. 2.—Seafloor photographs from the four sampling stations. White frame is 25 × 25 cm. **A)** Station Venice with abundant shell debris, small rhodolites, and two specimens of *Suberites domuncula* (red sponge) and *Cereus pedunculatus* in the upper part. **B)** Station Brijuni, muddy sediment surface with numerous dead mollusk shells (*Timoclea ovata?*) and few Lebensspuren. **C)** Station Piran 1, at center and lower left, pectinid shell fragments and a small burrow opening among abundant molluscan shell gravel; right, a large sponge aggregation. **D)** Station Piran 2, muddy sand with Lebensspuren and *Arca* sp. shell fragment close to orange sponge. Live pectinid on multispecies clump at outer right.

Brijuni archipelago became a Marine Protected Area (Fatovic-Ferencic 2006).

The two “Piran” stations are located in Slovenian waters a few km NW of the city of Piran. Station “Piran 1” is about 2.3 km from shore, at 22 m depth, within the protected perimeter of an oceanographic buoy operated by Marine Biology Station Piran (45.548867°N, 13.550900°E). Station “Piran 2” lies 2 km further away from shore, at a similar depth (22.7 m), in unprotected waters (45.563200°N, 13.537033°E). Both stations are characterized by muddy sand with a high proportion of shell debris and by the presence of epifaunal multi-species clumps mainly consisting of sponges and ascidians with a rich associated vagile fauna (ophiuroids, crustaceans, mollusks) (Fig. 2C, 2D).

Changes in molluscan composition at Piran 2 and Brijuni were analyzed by Mautner et al. (2018) and Schnedl et al. (2018).

Sampling

In summer 2013, at each station, three sediment cores were taken close to each other using an UWITEC piston corer with hammer action

(Gallmetzer et al. 2016). Core length was ~ 150 cm, and core diameter was 9 cm for the two cores designated for sediment and geochemical analyses, and 16 cm (or 9 cm, in the case of stiff sediments at the Venice and Brijuni stations) for the core intended for sieving and analysis of molluscan shell communities. This third core was sliced directly on board the coring vessel immediately after retrieval. The uppermost 20 cm were cut into 2-cm thick increments for higher resolution, and the rest of the core was cut into 5-cm thick increments. For better comparability of the surface section with the rest of the core, the 2-cm increments were pooled into 4-cm increments in geochronological and in some paleoecological analyses.

Analysis of Molluscan Assemblages

In the lab, core subsamples were sieved through a 1-mm mesh, and all the shells counted and identified to species level. For bivalves, only complete valves or fragments with preserved umbo were considered. The final count for each increment was achieved by adding the higher number of single valves (either right or left) to the number of articulated specimens.

TABLE 1.—List of functional and biocoenotic categories used to characterize the mollusk species observed. Table columns are independent of each other (categories within rows are unrelated). The feeding types “herbivorous”, “detritivorous”, and “chemosymbiotic” include mixed forms also capable of filter feeding. The listed abbreviations for biocoenoses follow the French nomenclature still widely used.

Feeding guilds	Weed-association	Biocoenoses	
herbivorous	strictly seagrass	AP	photophilic algae
detritivorous	mainly seagrass	DC	coastal detritic bottoms
filter feeding	rhizome layer	MI	unstable soft bottoms
carnivorous	lucinids	SVMC	muddy sands in sheltered areas
grazing	algae/seagrass	SGCF	coarse sands/fine gravels under bottom currents
scavenging	algae	HP	<i>Posidonia-oceanica</i> meadows
chemosymbiotic		VTC	coastal terrigenous muds
		SRPV	sediments protected from the influence of waves
		SFBC	fine, well-sorted sands
		C	coralligenous
		LEE	eurythermal and euryhaline lagoons
		DE	muddy detritic bottoms
		DL	offshore detritic bottoms

For gastropod shell fragments, the presence of the shell apex was the inclusion criterion. In analyses of absolute abundance, shell numbers from the 9-cm-diameter cores (stations Brijuni and Venice) were multiplied by 3.16 (the factor by which a 16-cm core increases in volume) to allow comparability of patterns in molluscan absolute abundances with the thicker cores from the Piran stations. We note that this extrapolation was not used in analyses of species richness. Similarly, in the molluscan core from Piran-2 station, where the increments from 10 to 35 cm and from 35 to 45 cm were split into quarters and half, respectively, due to high shell abundance, shell numbers were multiplied by four and by two, respectively, to account for comparable volumes. Molluscan species were assigned to functional categories with regard to feeding guild and weed-association (“weed” is used here as a general term for macroalgae and seagrasses) in order to capture down-core shifts in mollusk communities not only in terms of species turnovers and abundance trends but also on the functional level. Likewise, if possible, species were assigned to typical biocoenoses to allow for detection of biocoenotic changes in the cores (Table 1). A dataset listing down-core abundances and guild/biocoenosis assignments for each species, together with the literature used for ecological species characterization, is provided as an electronic supplement, Dataset S1, of the Online Supplemental Files.

Granulometry

One 9-cm-diameter core from each sampling station was used for granulometric analysis and for ^{210}Pb sediment dating. At the Venice station, this core was considerably shorter (only 85 cm) than the core used for mollusk shell analysis, most likely due to the presence of paleorelief between the two adjacent coring spots (fluvial clays occur on the bottom of both cores, marking the onset of the Holocene marine incursion). Core slicing followed the same procedure as for the molluscan core. From each core increment, a 10–20 g subsample was taken and screened through a set of five sieves (1 mm, 0.5 mm, 0.25 mm, 0.125 mm, and 0.063 mm). The fractions were dried and weighed, and the fraction < 0.063 mm was further processed using a SediGraph III 5120 Particle Size Analyzer following standard procedures. We defined four grain size classes: clay (< 0.002 mm), silt (0.002–0.063 mm), sand (0.063–2 mm), and gravel (2–63 mm). The sand was largely of terrigenous origin at Venice, whereas sand and gravel fractions consisted mainly of shells, shell fragments, and other biogenic material at the other stations.

Geochemical Analysis

A separate 9-cm core from each station was sealed after retrieval and further processed at the Institute of Marine Sciences in Venice (ISMAR) for geochemical analysis. First, radiographic images were taken of the intact cores to detect down-core density trends and to identify the core increments most suitable for subsample extraction and geochemical analysis. Then, in each core, 10 increments (only eight in the Venice core, which was shorter) were chosen, three within the uppermost 10 cm (0–2 cm, 4–6 cm, and 8–10 cm) and seven evenly spaced along the rest of the core, at depths slightly deviating between cores from individual stations. For each of these increments, three groups of sediment parameters were measured using the protocol described in Vidović et al. (2016): concentration of metals (Hg, Cu, Cr, Ni, Pb, As, Cd, Zn in mg/kg dry weight), concentration of nutrients (total carbon, total organic carbon, and total nitrogen, given in percentage of dry weight), and concentration of organic pollutants (polychlorinated biphenyls “PCBs” and polycyclic aromatic hydrocarbons “PAHs” in ng/g dry weight) (see Online Supplemental File, Dataset S2).

Geochronology

Core chronology is assessed with two different methods: ^{210}Pb dating of sediment, and radiocarbon-calibrated amino acid racemization (AAR) dating of mollusk shells.

^{210}Pb of Sediment.—In the uppermost 40 cm of each core, the activities of ^{210}Pb and ^{226}Ra were analyzed in 2-cm increments down to 20 cm core depth and in 5-cm increments down to 40 cm depth using a High Purity Germanium detector system. Apparent sedimentation rates were computed from the slope of excess ^{210}Pb according to the Constant Flux-Constant Sedimentation model (Sanchez-Cabeza and Ruiz-Fernández 2012). A surface mixed layer of 4–6 cm thickness at Piran and Brijuni with uniform or fluctuating ^{210}Pb -excess values was excluded from the computation of sedimentation rates. ^{210}Pb excess fell to supported values between 10 and 20 cm core depth where the decay profiles used in the slope estimation were terminated (Fig. 3). In the core from Venice station, the upper 10 cm (assigned here to the surface mixed layer) are characterized by ^{210}Pb excess values smaller than the down-core-declining values between 10–25 cm, and supported values appear for the first time below 60 cm.

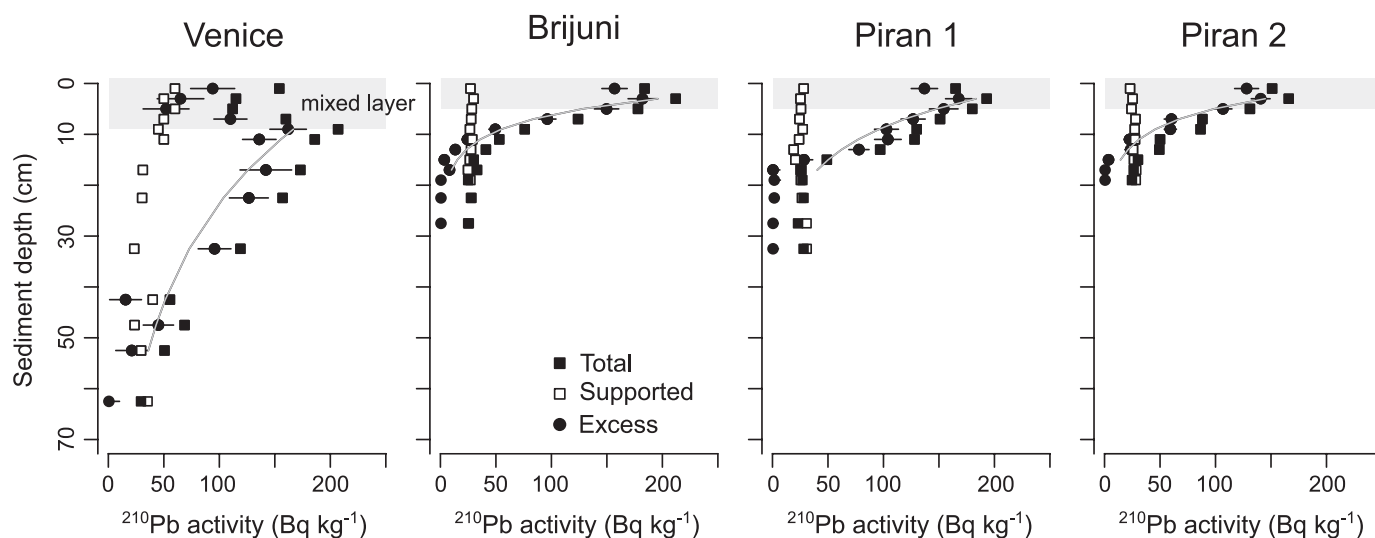


FIG. 3.— ^{210}Pb activity in sediment cores at the four sampling stations. Light gray rectangles represent zones with uniform or irregular excess ^{210}Pb activity. Gray lines represent the fitted decay profiles of excess ^{210}Pb .

Shell Dating.—From each of the four molluscan cores, a bivalve species occurring at high abundance throughout the core was used for shell dating by radiocarbon-calibrated amino acid racemization. This was the lucinid *Lucinella divaricata* for Venice, the venerid *Gouldia minima* for the two Piran stations (in addition, for Piran 2, shells of the corbulid *Corbula gibba* were dated), and the venerid *Timoclea ovata* for Brijuni. For *C. gibba*, the calibration is described in Tomašových et al. (2017), for *G. minima* in Tomašových et al. (2019), and for *T. ovata* in Schnedl et al. (2018). The calibration for *L. divaricata* is presented below.

The chronology of the Venice core is based on the shell ages of 341 specimens of *Lucinella divaricata* from 12 core increments (Online Supplemental File, Dataset S3), and of two specimens of the scallop *Aequipecten opercularis* collected in the 100–105-cm increment (Fig. 4). From 12 selected specimens of *L. divaricata*, shell parts were allocated for AMS ^{14}C dating. To avoid contamination, 30% of the outer shell mass was removed prior to AMS analysis in an ultrasonic bath and in 0.5M HCl, and treated in 15% H_2O_2 for 10 minutes, again in an ultrasonic bath (Goslar et al. 2004). Conventional ^{14}C ages were calculated using a correction for isotopic fractionation (Stuiver and Polach 2016). Conventional ages were converted to calendar years using Calib7.1 (Stuiver and Reimer 2006), the Marine13 calibration curve (Reimer et al. 2013), and a regional marine reservoir correction (ΔR) for the northeast Adriatic (Rovinj) equal to -61 years (standard deviation = 50 years) (Siani et al. 2000) (Table 2).

Small portions of the 347 dead and of three live-collected shells of *L. divaricata* were analyzed for the extent of amino acid racemization (AAR) at Northern Arizona University using reverse-phase high-pressure liquid chromatography (RP-HPLC, Kaufman and Manley 1998). Specimens were leached 20% by weight with a dilute solution of HCl and the resulting solutions were hydrolyzed at 110°C for six hours to release amino acids from their peptide chains. Concentrations and D/L values of aspartic acid (Asp), glutamic acid (Glu), serine (Ser), and alanine (Ala) were measured. Asp and Glu were used in age calibrations. Six specimens were flagged as outliers as described by Kosnik and Kaufman (2008) and removed from analyses.

We calibrated the rate of AAR in *L. divaricata* on the basis of the 12 ^{14}C -dated and three live-collected shells according to Allen et al. (2013). Asp and Glu D/L values were fit using four mathematical functions to model the relation between postmortem age and D/L values, and two uncertainty models (lognormal and gamma) using the R statistical computing language (R Core Team 2013). The four mathematical

functions include time-dependent rate kinetics (TDK), constrained power-law kinetics (CPK), simple power-law kinetics (SPK), and apparent parabolic kinetics. Each model was fitted with and without a non-zero initial D/L value. The time-dependent reaction kinetic model (TDK, Allen et al. 2013) for Asp D/L was the best model with the smallest BIC (Table 3), with the initial D/L value estimated from data (TDK1). This model was used in the final calibration. The calibration equation is $a \cdot \text{arctanh}([\text{DL} - \text{DL}_0]/[1 - \text{DL} \cdot \text{DL}_0])^b$, where DL is Asp D/L, DL_0 is Asp D/L at 0 years (here, 0.04479), and $a = 43589$ and $b = 2.342312$. The uncertainty is defined by the log-normal distribution, with the mean equal to log-transformed age estimate (in years) and the variance parameter of the log-normal distribution equal to 0.09134. AAR-calibrated calendar ages are set relative to the year of collection (2013 AD = year zero).

To summarize, between nine and 13 more or less evenly spaced core increments were chosen at each station (nine for Piran 1, eleven for Piran 2, 12 for Venice and 13 for Brijuni), and from each of these increments, ~ 30 specimens (complete valves or fragments with preserved umbo) were randomly selected for AAR analysis. Either only right or only left valves were used per increment to avoid double-dating of the same individual. In a few increments with lower shell abundance, both right and left valves had to be used. In total, 564 specimens of *G. minima* (Piran 1 and 2), 232 specimens of *C. gibba* (Piran 2), 300 of *T. ovata* (Brijuni), and 341 of *L. divaricata* (Venice) were used in shell-based core geochronology. AAR measurements were calibrated with ^{14}C ages of 13 specimens of *G. minima* (Tomašových et al. 2019), 12 of *L. divaricata* (this study), and 13 specimens of *T. ovata* (Schnedl et al. 2018), respectively. Median age and interquartile age range (corrected for calibration age error according to Dominguez et al. 2016) were computed for each increment. The increments with similar grain size, lithology, and proportion of major rock-forming components, including concretions, bryozoans, coralline algae, and mollusks were grouped into stratigraphic units. For each unit, 25th and 75th age percentiles and median age based on shell-age frequency distributions were computed (Table 4). Age distributions significantly overlap between some units, most likely due to bioturbation (Fig. 5). Therefore, geochronology of these units is better defined by age range (bounded by the 25th and 75th age percentiles) rather than by a single age estimate.

To compare long-term ecological trajectories among stations, core increments (2 or 5 cm thick layers) at each station were assigned to four phases using the sequence-stratigraphic terminology of model III of

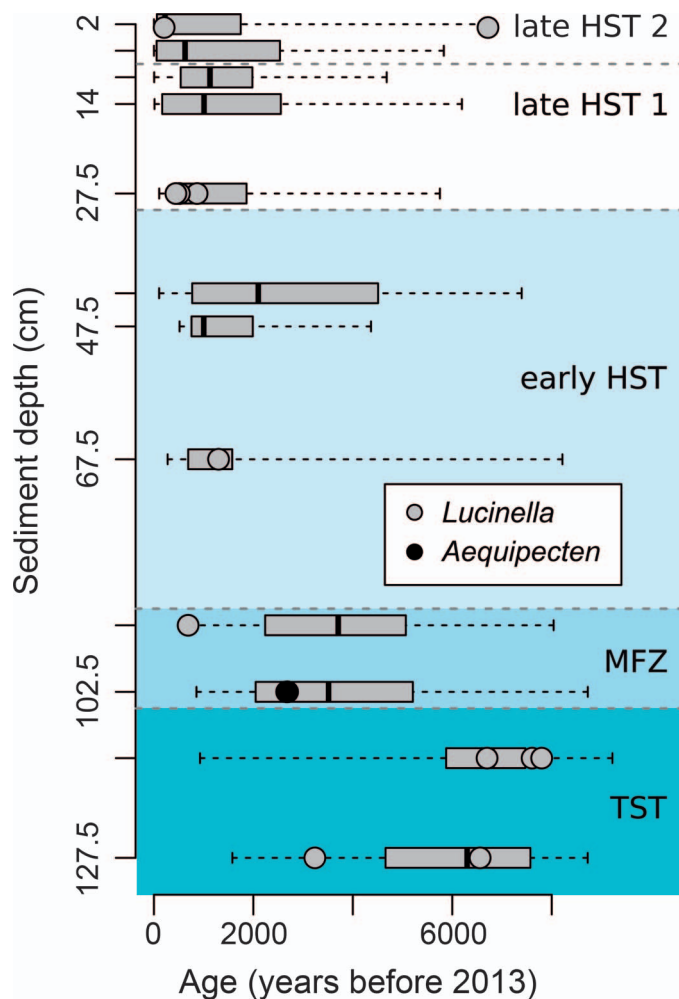


FIG. 4.—Radiocarbon ages and radiocarbon-calibrated amino acid racemization (AAR) ages of *Lucinella divaricata* (boxplots) at Venice station. Radiocarbon ages of individual shells are shown separately in gray (*L. divaricata*) and black circles (*Aequipecten opercularis*). Boxplots show median ages and 25th and 75th percentiles, whiskers denote age minima and maxima. Down-core changes in shell ages at Piran (*Gouldia minima*, *Corbula gibba*) and Brijuni (*Timoclea ovata*) are reported in Tomašových et al. (2019) and Schnedl et al. (2018).

Catuneanu et al. (2009) where the highstand phase terminates prior to the base-level fall (Hunt and Tucker 1992): (1) A transgressive phase (TST) ranging from the onset of the marine transgression about 10,500–11,000 years ago (at locations that are now at ~ 40 m depth; Storms et al. 2008) or 9,000 years ago (at locations now at ~ 20 m depth; Picone et al. 2008; Trincardi et al. 2011), correlating with the period of global sea-level rise, to the point of maximum flooding ~ 7,000 years ago (Antonioli et al. 2007; Vacchi et al. 2016; Amorosi et al. 2017); (2) A maximum flooding zone (MFZ) marking the maximum ingress and the transition from the late transgressive to the early highstand phase (~ 7,000–5,500 years ago; Trincardi et al. 2011; Amorosi et al. 2017) and documented by the establishment of shell beds with epifaunal bivalves at Brijuni and Piran; (3) An early highstand phase (eHST) lasting from the end of the transgressive phase to the onset of the stillstand (~ 2,000 years ago), coinciding with the beginning progradation of the Po, Isonzo, and Tagliamento Rivers (Amorosi et al. 2008; Zecchin et al. 2015; Amorosi et al. 2017), and with the appearance of distinct signs of human interference with the marine environment; and (4) A late highstand (effectively anthropogenic) phase (lHST) still underway, marking the era of pronounced marine ecosystem

changes induced by human activities in the recent past, including resource exploitation, pollution, and eutrophication (with recent oligotrophication since the 1990s; Mozetič et al. 2010; Djakovac et al. 2012).

Paleoecological Analysis

Environmental variables used in multivariate analyses of molluscan assemblage composition are represented by: (1) percentages of clay, silt, sand, and gravel; (2) sediment concentrations of Hg, Cu, Cr, Ni, Pb, As, Cd, and Zn; (3) concentration of total organic carbon (TOC); (4) concentration of total nitrogen (NT); and (5) concentrations of organic pollutants (PAHs and PCBs). These variables were log-transformed if not normally distributed, and z-standardized to account for different scales and units. Species diversity is given as (1) the observed number of species, and (2) true diversity or effective number of species (the exponential of the Shannon entropy, $\exp(H)$), which transforms the standard diversity index (H) into a linear scale representing the number of species in a perfectly even community (Jost 2007). Abundances were rarefied to a sample size of 150 individuals per increment, and, if necessary, extrapolated to this number according to Chao et al. (2014) using the R package “iNEXT” (Hsieh et al. 2016). Down-core differences in true diversity among the four phases are tested using the Wilcoxon rank test based on median effective species richness.

Differences in molluscan community composition between consecutive phases of individual cores are quantified by the pseudo-F statistics of permutational multivariate analysis of variance (PERMANOVA) (Anderson 2001). Non-metric multi-dimensional scaling (NMDS) based on Bray-Curtis distances (Ward and Hutchings 1996; Clarke and Warwick 2001) and fit to two dimensions is used to visualize changes or differences in mollusk community structure (1) between the four stations and (2) between five (Venice and both Piran stations) or six (Brijuni) stratigraphic units within stations (down-core changes). Bray-Curtis distances are based on square-root transformed relative abundances. Core increments with an overall mollusk shell abundance < 70 (Brijuni 0–4 cm, Venice 130–140 cm) and the increment 4–8 cm at Brijuni (outlier in the ordination of weed-association) were excluded from this analysis. Ordinations are performed not only for species abundances but also for abundances of ecological groups based on feeding type, weed-association, and biocoenotic affiliation.

To explore the sources of compositional variation in the ordination space, correlations between NMDS-axis scores and environmental variables were measured. The amount of community variation explained by environmental variables is quantified by redundancy analysis (RDA) based on a forward selection model (“ordi2step” function in R). Just as for the NMDS analyses, RDA is based on square-root transformed relative abundances—i.e., Euclidean distances used by RDA correspond to Hellinger distances, which are not sensitive to the double-zero problem, and are efficient in modeling species responses to short environmental gradients (Legendre and Gallagher 2001; Legendre and De Cáceres 2013). We note that constrained analyses of principal coordinates based on Bray-Curtis distances generate very similar results. The application of RDA, however, is limited to those ten core increments (eight in the core from Venice station) for which measurement data of environmental variables are available. To compare the proportion of compositional variation explained by stratigraphic differences within the four stations (defined by sediment depth of a given assemblage, at the scale of 5-cm increments) with the amount explained by geographic differences among the stations (defined by latitude and longitude of each station), we extend redundancy analysis to variation partitioning based on Hellinger distance (Peres-Neto et al. 2006). Statistical analyses were performed in R-studio (version 3.1.3.) using the “vegan” package (Oksanen et al. 2016). The R-code and two related input files are accessible in the supplementary material.

TABLE 2.—Numerical ages of 12 dead-collected and three live-collected specimens of *Lucinella divaricata* used in AMS-AAR calibration with D/L of aspartic acid (Asp) and glutamic acid (Glu). The specimen ID corresponds to the unique specimen identification number, Poznan ID is the unique identification number for the radiocarbon analyses from the Poznan Radiocarbon Laboratory, Poland. The calibrated age (yr) is relative to 2013 AD, the year of sampling.

Specimen ID	Poznan ID	Conventional ¹⁴ C age	Conventional ¹⁴ C age error (2 s.d.)	Calibrated age (to 2013 AD)	Lower 95% conf. bound on calibrated age	Upper 95% conf. bound on calibrated age	Asp D/L	Glu D/L
Ven M38 0-2 001	Poz-71706	6150	64	6718	6881	6548	0.414	0.174
Ven M38 2-4 016	Poz-71710	455	58	206	318	64	0.126	0.034
Ven M38 25-30 001	Poz-71711	1200	58	869	980	747	0.255	0.067
Ven M38 25-30 016	Poz-71712	760	58	513	594	377	0.206	0.058
Ven M38 25-30 020	Poz-71944	680	58	443	546	341	0.158	0.051
Ven M38 65-70 002	Poz-71945	1620	58	1300	1413	1165	0.287	0.068
Ven M38 90-95 001	Poz-71946	1000	58	689	784	589	0.219	0.053
Ven M38 110-115 003	Poz-71948	6135	61	6699	6849	6538	0.477	0.173
Ven M38 110-115 005	Poz-71949	7000	64	7605	7717	7492	0.458	0.158
Ven M38 110-115 009	Poz-71950	7210	64	7798	7938	7661	0.497	0.182
Ven M38 125-130 001	Poz-71952	3265	58	3237	3399	3065	0.377	0.106
Ven M38 125-130 007	Poz-71953	6010	61	6559	6709	6410	0.441	0.158
Venice (V-1)				1	2	0.1	0.054	0.018
Venice (V-2)				1	2	0.1	0.055	0.017
Venice (V-3)				1	2	0.1	0.058	0.019

RESULTS

Stratigraphy and Down-core Changes in Sediment Composition

The sampling regions covered by the four sediment cores (NE, SE, and central-western part of the northern Adriatic Sea) represent different depositional environments and stratigraphic histories. Only the two cores from the neighboring Piran stations show similarities in the stratigraphic distribution of percentages of sand and gravel, and in the degree of shell packing.

Venice.—At the bottom of the Venice core, the Holocene transgressive surface is marked by a sudden change from dark, organic-rich fluvialite or paralic clays to marine sediments containing shells of both marine and freshwater species. The sediment consists almost exclusively of pure, well-sorted siliciclastic sands throughout the core (Fig. 6). The down-core age distribution of *L. divaricata* shells (Fig. 4) shows that median ages of this species range between 200 and 1,100 years in the upper 30 cm, between

900 and 2,100 years at 40–70 cm, between 3,500 and 3,700 years at 90–105 cm (¹⁴C ages of two specimens of *Aequipecten* are equal to 2,700 years), and between 6,300–6,800 years at 110–130 cm. The interquartile ranges of *L. divaricata* ages (corrected for age error) in 5-cm increments span ~ 500 to 2,000 years. Considerable sediment mixing is suggested by similarities in median ages of 5-cm increments within the five stratigraphic units. Down-core changes in median *L. divaricata* ages thus indicate that net sedimentation rates were small (~ 0.01–0.05 cm/year) during the entire Holocene period. An abrupt shift in median age between 100–105 and 110–115 cm from 3,500 to 6,300 years indicates a major hiatus in sediment accumulation. Fitting the ²¹⁰Pb excess values against sediment depth at 10–50 cm indicates that apparent sedimentation rates are 0.88 cm/year, much higher than estimates based on down-core changes in median ages of *L. divaricata* over the same stratigraphic interval (~ 0.05 cm/y, with median shell age equal to 1,000 years at 45–50 cm).

The Venice core can be subdivided into four units based on down-core changes in the composition of biogenic sediments (Fig. 7): (1) In the

TABLE 3.—Calibration statistics for the rate of amino acid racemization (AAR) based on paired AAR and radiometric analyses of *Lucinella divaricata* and two models of uncertainty, showing models with Bayes Information Criterion (BIC) values less than six units relative to the model with minimum BIC. Abbreviations and explanations: APK = apparent parabolic kinetics; CPK = constrained power-law kinetics; SPK = simple power-law kinetics; TDK = time-dependent reaction kinetics; 0 = the initial D/L value is fixed at zero; 1 = the initial D/L value is estimated from data, a-d = model parameters, R0 = the D/L value at time of death.

Amino acid	Model	ln(a)	ln(b)	c	log(R0)	ln(d)	BIC	ΔBIC
Gamma uncertainty								
Glu	APK1	12.5450294	NA	-0.0424827	-4.8021627	4.36828276	199.04	0.00
Glu	TDK1	12.0410377	0.54289118	0.88189243	-4.2839274	4.12519838	199.23	0.19
Glu	SPK1	12.357917	0.67625903	1.57770102	-4.1335673	4.133904	200.38	1.34
Glu	APK0	12.4085925	NA	NA	NA	5.06409473	202.44	3.40
Glu	SPK0	12.8029124	0.79295997	NA	NA	4.73799327	203.06	4.01
Glu	TDK0	12.7408809	0.78099925	NA	NA	4.80893148	203.31	4.27
Asp	SPK1	11.1001772	1.07202452	NA	NA	4.40793196	203.69	4.65
Asp	TDK0	10.6936588	0.98240096	NA	NA	4.5861671	203.71	4.67
Lognormal uncertainty								
Asp	TDK1	10.6825629	0.85113851	0.95175147	-3.1058379	-2.393191	197.63	0.00
Asp	APK1	10.3527626	NA	1.36845229	-3.0082423	-2.090888	201.31	3.67

TABLE 4.—Core depth and age range of stratigraphic units and depositional phases in the molluscan cores from the four sampling stations. Median age refers to median age estimates for 4–5 cm-thick increments based on *T. ovata*, *G. minima*, *C. gibba*, and *L. divaricata*. The empirical 25th and 75th age percentiles are estimated based on ages in the whole units, and ages in parentheses are informed based on ages of other bivalves (*Arca noae*, *Ostrea* sp., *Glycymeris glycymeris*, *Aequipecten opercularis*, *Chlamys varia*).

Core	Phase	Stratigraphic unit	Median age per unit (y)	25–75 th Quantiles per unit (y)	Lower boundary determined by
Venice (based on <i>Lucinella divaricata</i> , additional dates from <i>Aequipecten</i>)					
0–8 cm	IHST 2	1	<620	<2000	
8–30 cm	IHST 1	2	870–1100	300–2500	
30–90 cm	eHST	3	1000–2100	1000–2100	
90–105 cm	MFZ	4	3500–3700	2100–5100	
105–135 cm	TST	5	6300–6900	4900–7500 (9000)	oldest <i>Lucinella</i> shells
Brijuni (based on <i>Timoclea ovata</i> , additional dates from <i>Glycymeris</i> , <i>Aequipecten</i> , <i>Chlamys</i> , <i>Ostrea</i> , and a plant remnant)					
0–10 cm	IHST 2	1	<200	<370	
10–20 cm	IHST 1	2	300–600	200–1700	
20–50 cm	eHST 2	3	2100–2600	1500–3600	
50–90 cm	eHST 1	4	3200–4300	2900–4600	
90–120 cm	MFZ	5	4900–5200	4500–6100 (7500)	<i>Glycymeris</i>
120–160 cm	TST	6	5000–6100	4800–6800 (11,350)	plant remain
Piran 1 (based on <i>G. minima</i> , additional dates from <i>Arca</i> and <i>Ostrea</i> , but not from <i>Corbula gibba</i>)					
0–8 cm	IHST	1	<1200	<1900	
8–16 cm	eHST	2	1000–3100	1000–3100	
16–35 cm	MFZ	3	4700	3100–4500 (6500)	<i>Ostrea</i>
35–65 cm	ITST	4	4700–4800	4100–5500 (7500)	<i>Ostrea</i>
65–150 cm	eTST	5	4500–6000	4200–6000 (9500)	oldest <i>Gouldia</i> shells
Piran 2 (based on <i>G. minima</i> and <i>C. gibba</i> , additional dates from <i>Arca</i> and <i>Ostrea</i>)					
0–8 cm	IHST	1	<1100	<1800	
8–16 cm	eHST	2	1500–3500	1100–3100 (5100)	<i>Arca</i>
16–35 cm	MFZ	3	3800–5800	3400–5800 (6500)	<i>Ostrea</i>
35–65 cm	ITST	4	4100–6400	3600–6700	
65–150 cm	eTST	5	4500–8600	4800–8000 (10,400)	oldest <i>Corbula</i> shells

deepest part (135–105 cm) representing the TST, in addition to the dominant molluscan and rhodolitic fragments, foraminiferal tests of the species *Ammonia* cf. *beccarii* and *Massilina* cf. *secans* and carbonate concretions are abundant. Remains of fresh-water gastropods are frequent, mainly opercula of the genus *Bithynia*, reflecting pre-transgression freshwater or brackish environments; (2) Between 105 and 90 cm (MFZ), *A. cf. beccarii* and *M. cf. secans* decrease markedly in abundance; in shallower core depths, they are completely absent. Carbonate concretions are larger compared to the TST; (3) The unit between 90 and 30 cm (eHST) is characterized by a high abundance of the small irregular sea urchin *Echinocyamus pusillus*; and (4) In the uppermost unit (IHST), from 30 cm up to the surface, the molluscan gravel co-occurs with numerous branched rhodolites, which are also a constituent part of the living assemblage (Fig. 2A).

Brijuni.—A dated terrestrial plant fragment from the base of the Brijuni core is ~ 11,350 years old. The median age of *Timoclea ovata* shells from dated increments increases monotonically down-core, ranging from 160 years at 0–4 cm core depth to 6,100 years at 150–155 cm (Fig. 5), and a maximum shell age of 10,100 years. Net sedimentation rates based on differences in median ages of *T. ovata* between increments range between ~ 0.01–0.04 cm/year. Interquartile age ranges (corrected for age error) of *T. ovata* in 5-cm increments range mainly between 500 and 1,000 years. The core is stratigraphically subdivided into six units: the TST at the bottom of the core (160–120 cm), the MFZ represented by a shell-bed at 120–90 cm with shells heavily coated by encrusting bryozoans (large ¹⁴C-dated shells of *Arca*, oysters and *Glycymeris* from this shell bed span between 5,500 and 7,800 years; Schnedl et al. 2018), an eHST with coarser sediment in the lower and finer sediment in the upper part (90–50 cm and 50–20 cm, respectively), and an IHST (or “anthropogenic” phase, 20–0 cm) at the core top, with the uppermost 10 cm enriched in organic pollutants,

total nitrogen, and total organic carbon. Grain size composition changes strongly up-core, with a large proportion of molluscan gravel in the lower part, bryozoan-molluscan sand in the upper part, and a higher contribution of coralline algae in the uppermost part (Figs. 6, 8). The overall trend is fining upward, with sediment-starved conditions at the bottom of the core during the marine transgression phase, and a marked shell bed with encrusted large bivalves between 120 and 90 cm. As in the Venice core, shells of terrestrial (nine species) and freshwater (15 species) gastropods are abundant in the TST but decrease steadily up-core. Molluscan sand and gravel peak between 130 and 95 cm core depth, with a maximum percentage of ~ 80%, and then gradually decrease upwards. In the uppermost 20 cm, silt and clay constitute ~ 80% of the sediment. According to ²¹⁰Pb sediment dating, the apparent sedimentation rate during the deposition of increments between 4 and 16 cm core depth has been ~ 0.15 cm/year, exceeding the estimates of sedimentation rate based on down-core changes in median ages of *T. ovata* by one order of magnitude. Sand and gravel, in this core, are mostly of biogenic origin and consist mainly of molluscan shell hash, exoskeletal parts of crustaceans (present mainly in the deeper core sections), and bryozoan colony fragments. Bryozoans increase in abundance from 90 cm up to the surface, showing a gradual up-core shift from encrusting to bushy (*Cellaria* spp.) growth forms. The bivalve shell bed between 120 and 90 cm depth consists of large, strongly bored shells of glycymeridids, scallops, and oysters, with common encrustation by coralline algae, serpulids, and bryozoans (Fig. 8).

Piran 1 and Piran 2.—Five stratigraphic units can be distinguished at the Piran stations (Mautner et al. 2018; Tomašových et al. 2019). In contrast to Venice and Brijuni, the TST unit is more expanded and the HST units are very thin. Stratigraphic mixing coupled with a temporally disjunct production of two species (e.g., Broecker et al. 1999) generates significant age offsets between median ages of *Gouldia minima* and *Corbula gibba* in

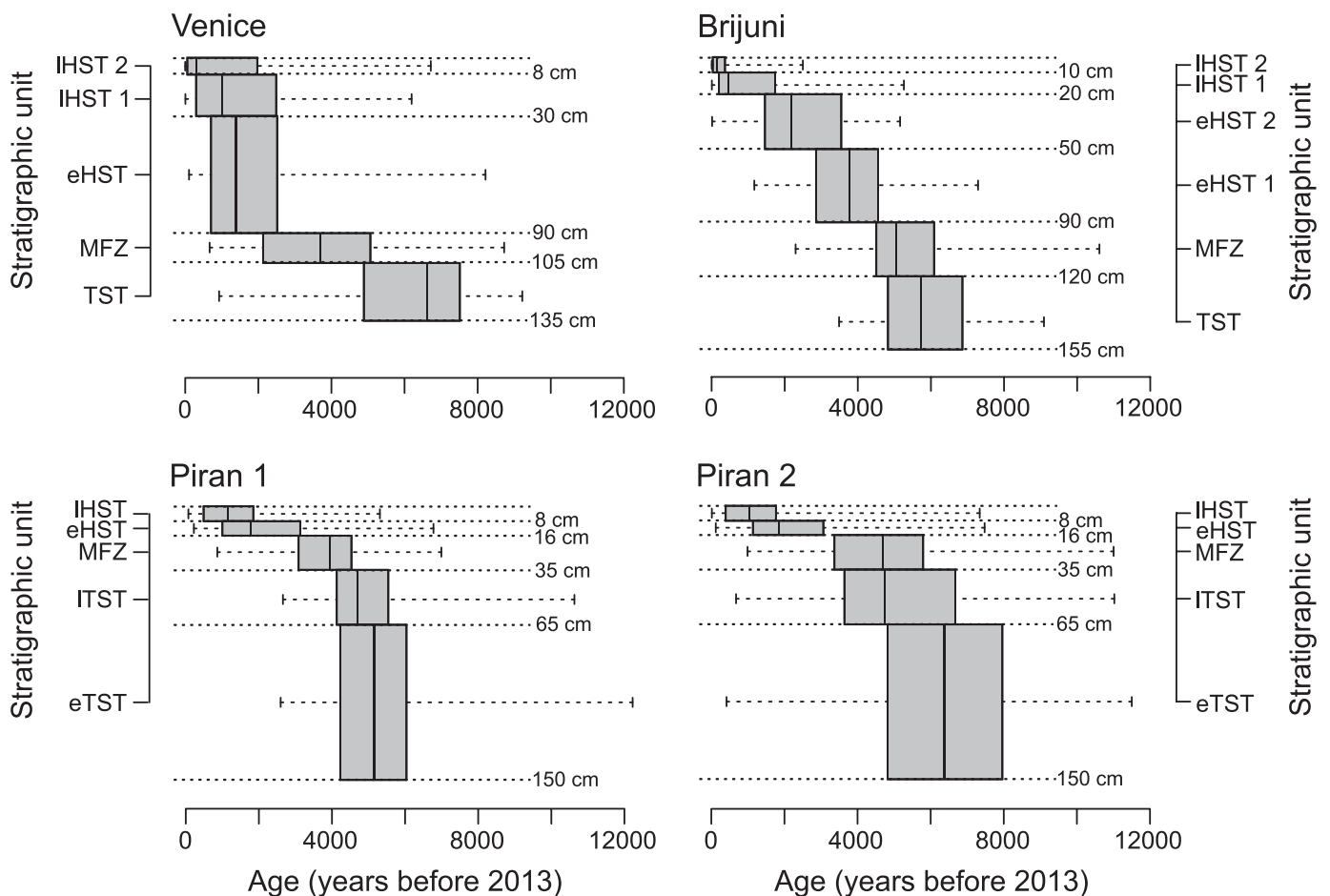


FIG. 5.—Boxplots showing median ages and the 25th and 75th age percentiles (and total ranges) of stratigraphic units at four stations. The width of boxes along the y-axis is scaled according to sediment thickness of these units.

the same increments (Tomašových et al. 2019). At Piran 1 and 2, the median age of *G. minima* shells increases steadily down-core from ~1,000 years at 0–4 cm to ~5,000–6,500 years at 90–100 cm, and then it remains relatively constant down-core. In contrast, the median age of *C. gibba* increases from ~1,000 years at 0–4 cm to ~7,000–8,000 years at 90–100 cm. Similar to Venice and Brijuni, the cores can be split into five major stratigraphic units based on changes in grain size: (1) the early TST at 65–150 cm formed by muddy sand; (2) the late TST formed by molluscan sand and initial oyster-rich levels at 65–35 cm; (3) the MFZ formed by the lower part of a shell bed (mainly oysters) at 35–16 cm; (4) the eHST corresponding to the upper part of the shell bed (mainly *Arca noae*) at 16–8 cm; and (5) the IHST represented by the topmost 8-cm-thick molluscan sandy mud.

Stations Piran 1 and Piran 2 show similar grain size composition and stratigraphy despite being ~2 km apart. Both stations share a coarsening-upward trend in grain size and an up-core increase in average shell size (Fig. 6; Mautner et al. 2018). The proportion of mud in the deeper part of the core (150–75 cm) is 70–80% and decreases to less than 20% in the uppermost 25 cm in favor of a sand and gravel fraction consisting mainly of mollusk shells, with the addition of echinoderm and crustacean fragments and foraminiferal tests. At both stations, the deepest core intervals (155–135 at Piran 1 and 145–135 at Piran 2) contain a high number of *Modiolus cf. adriaticus*. The densely packed shell bed with large shells of epifaunal bivalves (*Arca noae*, *Ostrea* sp., *Modiolus* sp.) between 8 and 35 cm is a distinct feature in both cores (Fig. 9). The

uppermost 8 cm consist of molluscan sands with dispersed coralline algae (*Lithothamnion* spp.), which locally expose the shells of the underlying shell-bed-building species at the sediment surface (Fig. 2C, 2D). At Piran 1, a loosely packed shell bed is preserved between 95 and 35 cm, formed by ostreid and mytilid shells (*Ostrea* sp. and *Modiolus* sp.). As at Venice and Brijuni stations, single-species interquartile age ranges at the Piran stations range mainly between 1,000–2,000 years (Tomašových et al. 2019). The average sedimentation rate based on the excess ²¹⁰Pb profiles between 4–14 cm amounts to 0.29 cm/y at station Piran 1 and 0.16 cm/y at Piran 2, again significantly exceeding the net sedimentation rates indicated by down-core changes in median age of *G. minima* and *C. gibba* in the upper 20 cm (Tomašových et al. 2019).

Geochemistry

Sediment contamination with heavy metals and organic pollutants increases upwards at all stations, with marked peaks in the uppermost 20 cm (Fig. 10). The strongest contamination is observed at Brijuni, the lowest at Venice. The measured concentrations exceed NOAA benchmark values (Long et al. 1995) in several cases: Hg concentrations at Brijuni are higher than Effects Range-Median (ERM) level (at Piran 2, they are close to this threshold); Zn exceeds Threshold Effects Levels (TEL) values at all stations except for Venice. Pb, PAH and PCBs concentrations are below benchmark values at all stations, but clearly increase in the uppermost increments. TOC and TN concentrations increase in the uppermost 10–20

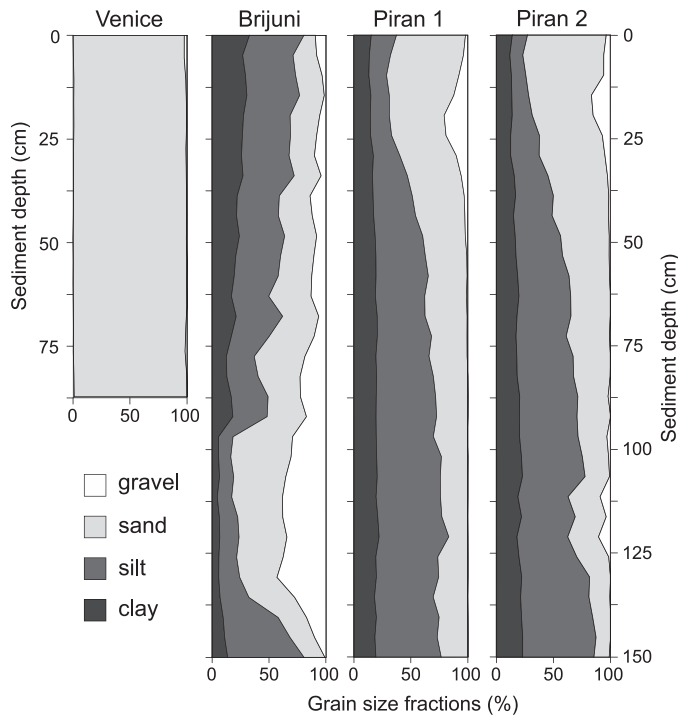


FIG. 6.—Grain size composition at the four sampling stations. At Venice, the marine sediment column in the core used for sediment analysis was shorter (85 cm) than in the other cores, probably due to the presence of a paleorelief. Note the opposite up-core trend in grain size proportions between Brijuni (fining upward) and the two Piran (coarsening upward) stations.

cm at Brijuni and Piran 1 (at Piran 2, only total nitrogen increases upwards), whereas at Venice they remain low.

Molluscan Density, Species Richness, and Diversity

The four sediment cores yielded ~98,700 shells from 52,710 mollusk individuals belonging to 341 different species, including 180 gastropods, 120 bivalves, 9 chitons, five scaphopods, and 27 non-marine mollusks (17 freshwater and 10 land snail species). The highest density (individuals per 100 cm³) occurs in the eHST of the two Piran cores (upper part of the shell bed, maximum 618 ind/100 cm³ at Piran 2 and 314 ind/100 cm³ at Piran 1) and in the TST of the Venice (231 ind/100 cm³) and Brijuni cores (430 ind/100 cm³) (Fig. 11A).

Stratigraphic changes in mollusk density at the Piran stations on one hand and at Brijuni/Venice on the other hand show opposite trends: At Piran, density is relatively constant below 80 cm core depth, rises slowly from this point upwards, and experiences a burst above 40 cm. At Venice and Brijuni, the highest density occurs in the lowermost part and then decreases continuously up to the top. All cores except for the Venice station display a sudden density drop in the uppermost 10 cm. In all cores, the raw species richness (Fig. 11B, 11C) increases steeply immediately above the transgressive surface. At Venice and Brijuni, it peaks around 120 cm core depth (90–100 species). At Venice, raw species richness decreases slightly and stabilizes at ~50 species around 60 cm depth without major changes up to the surface. At Brijuni, high species richness extends up-core until ~40 cm depth, from where it declines, with a sharp drop in the uppermost 12 cm. At the two Piran stations, after a first steep increase in the early TST, raw species richness grows steadily up-core with minor fluctuations until the near-surface unit (maxima: 116 species at Piran 2 and 120 species at Piran 1) where, similar to the other stations, a sudden decline sets in, which is more pronounced at Piran 1 than at Piran 2.

Effective number of species ($\exp(H)$) is highest at Brijuni station (median: 30), followed by Venice (28), Piran 2 (25), and Piran 1 (24) (Fig. 11D). Here, the most conspicuous stratigraphic trends are an extensive peak in the MFZ with subsequent sharp drop in the eHST at Brijuni, and a marked drop in the uppermost 30 cm in both Piran cores. This sudden diversity loss at Piran significantly distinguishes the HST phases from the MFZ and the TST at both stations (Table 5). At Brijuni, the effective number of species is significantly higher in the eHST than in the MFZ/TST; in the IHST, diversity drops again to low values similar to the MFZ. At Venice, diversity fluctuates considerably throughout the core without significant pairwise differences between the four units (Table 5). A diversity comparison between the same stratigraphic units in all four cores does not show any significant differences between the Piran cores and only partial differences between Piran and the two other stations and between Brijuni and Venice. Differences concern mainly the early and late HST phase and are determined by the marked diversity loss in the uppermost increments at Piran and the diversity increase during eHST at Brijuni station (Online Supplemental File Table S4).

Down-Core Trends on the Species, Functional and Biocoenotic Level

Venice.—The lucinid bivalve *Lucinella divaricata*, which occurs preferentially in sediments of seagrass meadows is the most frequent species throughout the core (Fig. 7). Absolute abundances of this species are much greater in deep than in shallow units, indicating particularly suitable habitat conditions during the TST and the MFZ. The existence of seagrass environments during this period is supported by the strictly seagrass-associated rissoid gastropods *Rissoa monodonta* and *R. membranacea*, which occur exclusively in the TST below 100 cm core depth. The core is further dominated by the epifaunal bivalves *Anomia ehippium* and *Aequipecten opercularis* that peak at 90–95 cm, the infaunal bivalve *Donax venustus* reaching a maximum in the TST, and by the tellinid *Moerella distorta* peaking at 60–65 cm. From the MFZ upwards, epifaunal species slightly decline and infaunal species associated with sandy bottoms increase in abundance (e.g., *Tellina* spp.). *Parvicardium minimum* becomes the second most abundant species, and the abundance of *Glycymeris glycymeris*, a species characteristic of sandy bottoms exposed to currents, increases from the MFZ onwards. In addition, in the intermediate core section, a slight increase of deposit feeders can be observed. In the IHST, the ratio between infaunal (the dominant type of substrate relation) and hard-bottom epifaunal species remains largely constant while, in terms of feeding guilds, deposit feeders decline in favor of filter feeders. Overall, this core is characterized by a high abundance of seagrass-associated species in the TST and by species adapted to well-sorted, nutrient-poor sands in the HST phases. This is also reflected in the biocoenotic structure, with a dominance of species from the detritic community and important proportions of representatives from the biocoenoses associated with photophilic algae and fine, well-sorted sands (AP, SRPV, and SFBC; see Table 1). The community appears relatively homogenous over wide sections of the core, and down-core changes on the functional or biocoenotic level are not particularly marked (Table 5), possibly due to pronounced mixing processes that generated highly time-averaged assemblages.

Brijuni.—The TST and the MFZ are dominated by epifaunal (e.g., *Striarca lactea*) and vegetation-associated mollusks, of which a large proportion (61%) is strongly but not exclusively related to seagrasses (e.g., *Alvania geryonia*, *Alvania cimex*, *Rissoa violacea*) (Online Supplemental File Fig. S5). A shell bed with large shells of oysters, scallops, and glycymeridids heavily coated by encrusting bryozoans characterizes the MFZ (Fig. 8). Above this shell bed, erect bryozoans abruptly become a constitutive part of the biogenic gravel, and seagrass-associated species decline in favor of species with a preference for algae. Infaunal (e.g.,

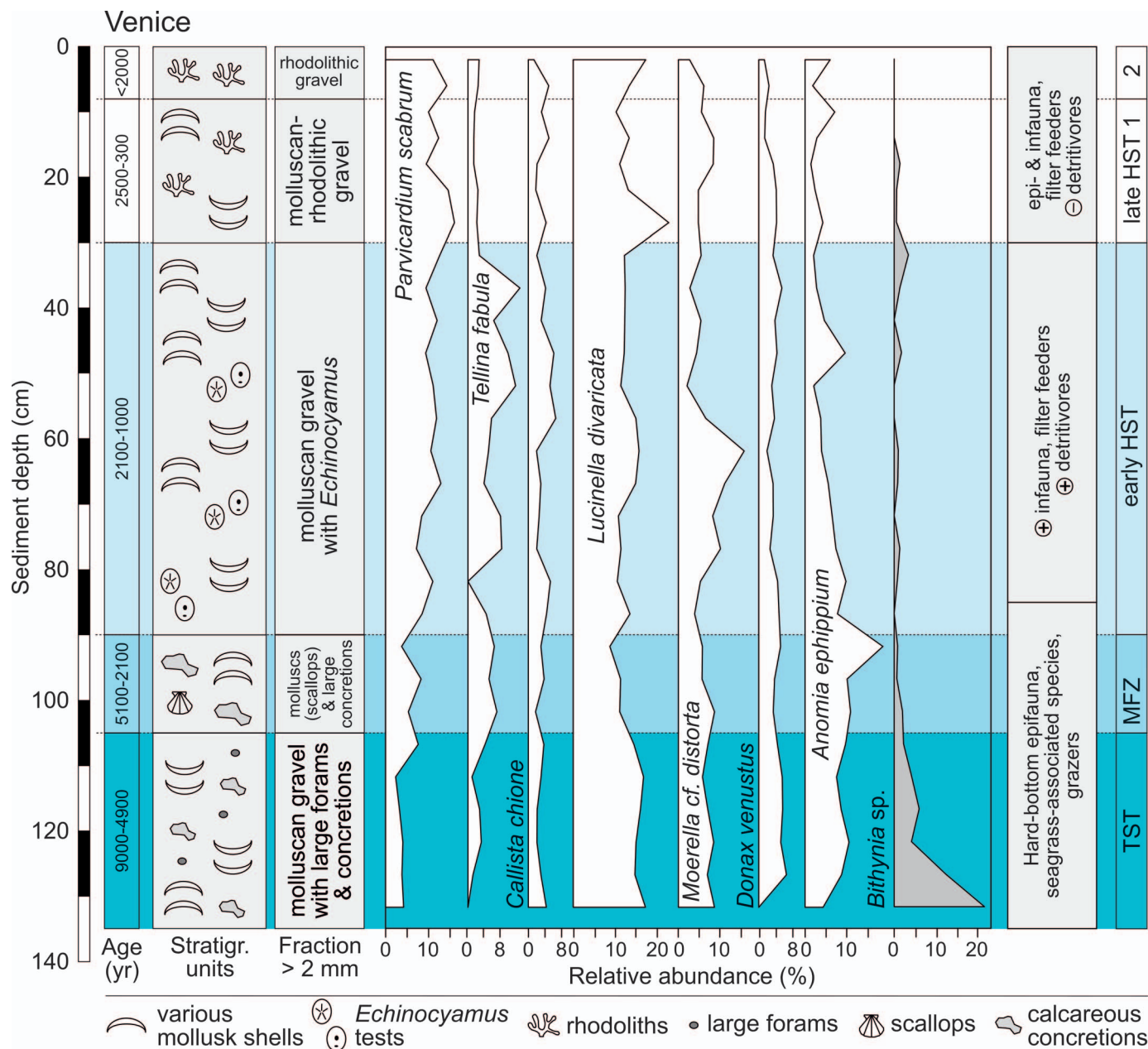


FIG. 7.—Stratigraphic section, relative abundances of the dominant species sorted according to their weighted average, and most important functional down-core trends (right side) in the Venice core. Y-axis is given as depth and time axis, major core units are indicated at the outer right and highlighted in different colors in the background. Freshwater species (*Bithynia sp.*) in gray. Age range of stratigraphic units is primarily defined by the 25th and 75th percentiles of shell ages (Table 4).

Timoclea ovata, *Parvicardium* spp.) and epifaunal species typical of detritic bottoms (e.g., *Bittium submammillatum*, *Jujubinus montagui*, *Anomia ephippium*) dominate the community in the eHST. In the IHST, the proportion of epifaunal mollusks drops rapidly while infaunal species such as *Nucula nucleus* and *T. ovata* further increase. Besides filter feeders (the dominant feeding guild in this core), 20–40 % of all mollusk species are grazers. However, this feeding type experiences a drastic decline in the uppermost 30 cm, which is compensated by a rise in detritivore and filter-feeding species (Fig. 8). In biocoenotic terms, the mollusk community at Brijuni is best described as a coastal detritic community with a large proportion of vegetation-associated species and some representatives of the coralligenous biocoenosis and the current-swept, coarse sands (SGCF). Significant biocoenotic shifts are observed between the lower part of the

core (TST and MFZ), the eHST1, and the upper core section (eHST2 and IHST) (Fig. 12B, Table 5), possibly due to a larger number of species characteristic of muddy sands in sheltered areas (SVMC) in the eHST1 and the lack of species typical for coastal terrigenous muds (VTC) in the bottom and top units of the core (Online Supplemental File Fig. S6).

Piran 1 and 2.—The mollusk communities of the two Piran cores follow highly similar trends. The most abundant species are *G. minima* and *C. gibba*, two filter-feeders with an infaunal and semi-infaunal life habit, respectively, characteristic of muddy or muddy-sandy bottoms. Relative abundances of the two species show opposite up-core trends: *C. gibba* is more abundant in the early TST, where it constitutes up to 20% of the whole community, and *G. minima* in units with coarser sediments, from the

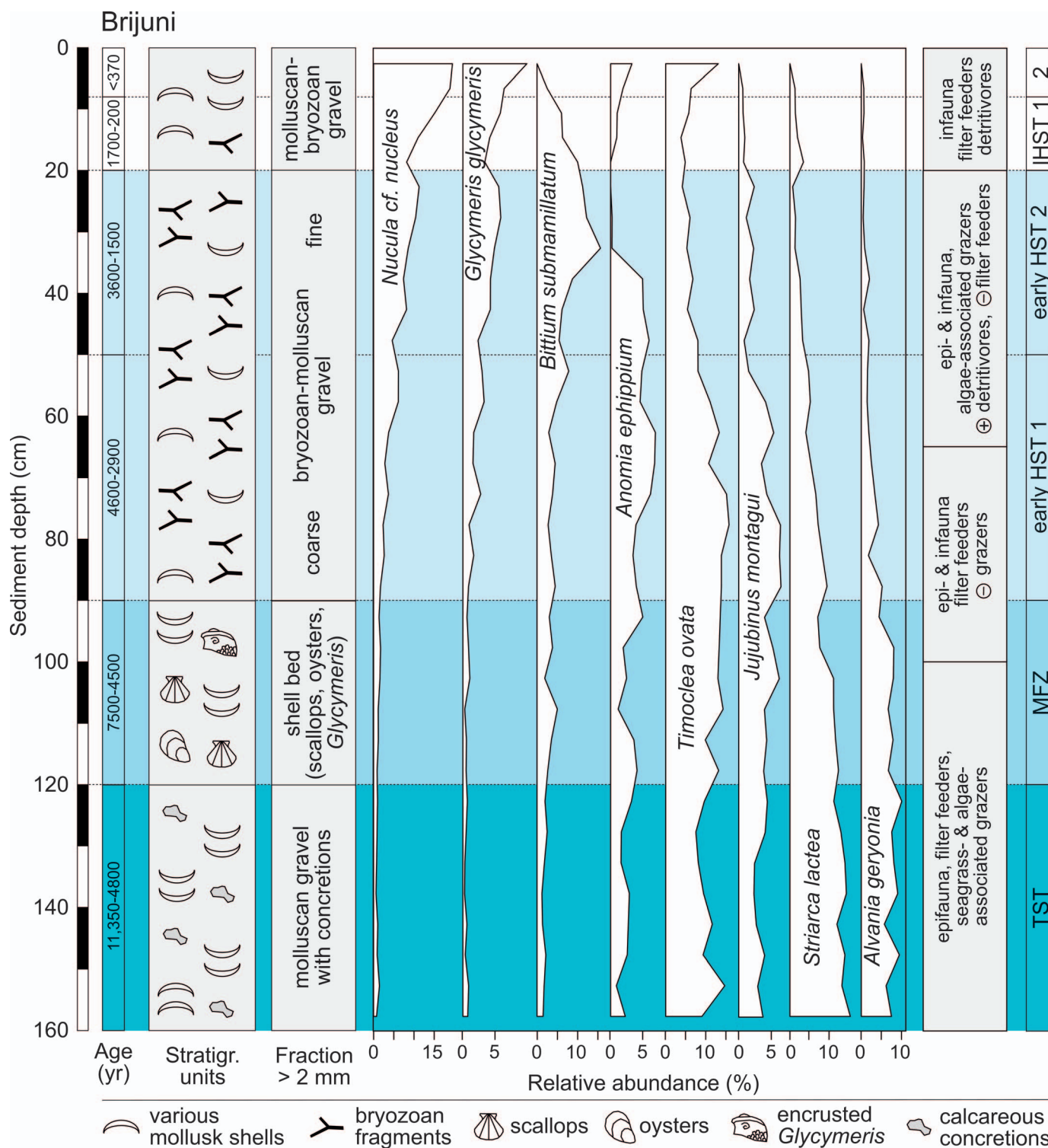


Fig. 8.—Stratigraphic section, relative abundances of the dominant species sorted according to their weighted average, and most important functional down-core trends (right side) in the Brijuni core. Y-axis is given as depth and time axis, major core units are indicated at the outer right and highlighted in different colors in the background. Age range of stratigraphic units is primarily defined by the 25th and 75th percentiles of shell ages (Table 4).

late TST up to the surface (Fig. 9). In the early TST, the mollusk community is dominated by infaunal and epifaunal filter feeders and detritivores typical of muddy bottoms (in addition to *C. gibba*, e.g., *Abra alba* and *Flexopecten glaber*). A third important feeding guild, grazers, is

represented by several gastropod species associated with algae and/or seagrasses (e.g., *Pusillina* spp. and *Bittium* spp.). Following the coarsening-upwards trend, the dominance of infaunal species recedes up-core in favor of epifaunal species (Fig. 9). At Piran 1, this trend leads to the

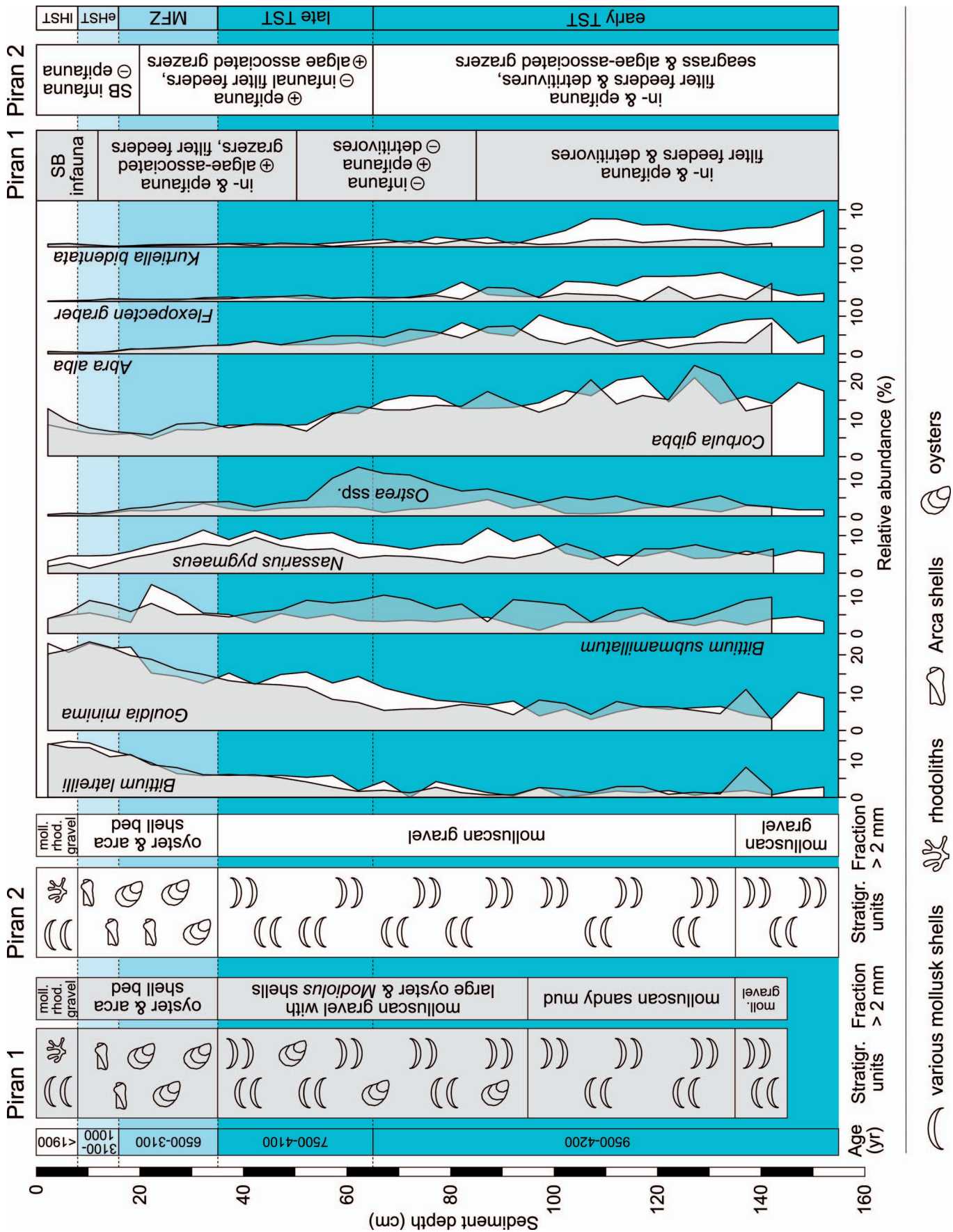


Fig. 9.—Stratigraphic profile, relative abundances of the dominant species sorted according to their weighted average, and most important functional down-core trends (right side) for the stations Piran 1 (gray) and Piran 2 (white). One of the main differences between the two stations are traces of a mollusk shell bed between 95–35 cm only at Piran 1. Age range of stratigraphic units is primarily defined by the 25th and 75th percentiles of shell ages (Table 4).

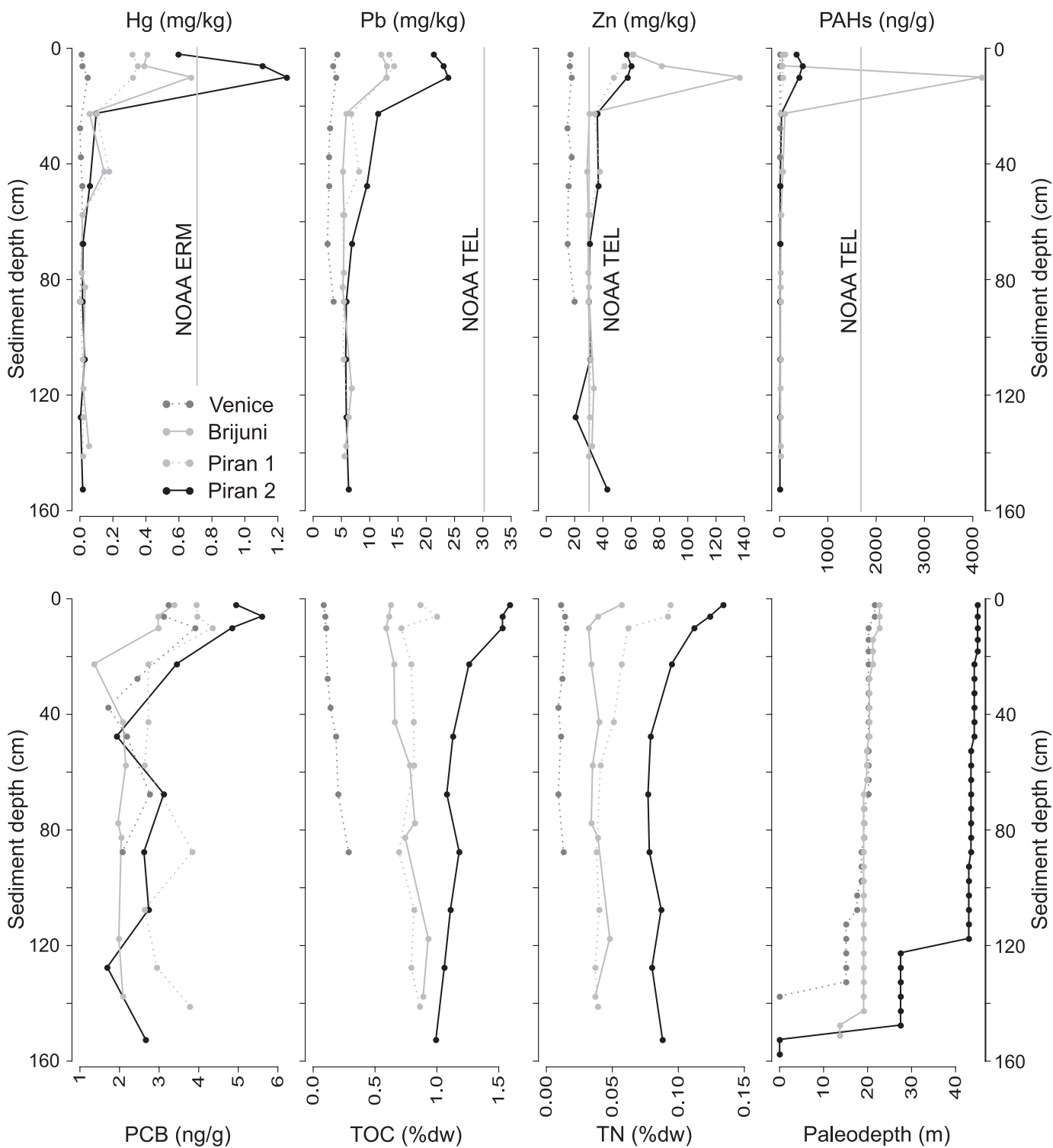


FIG. 10.—Concentrations of heavy metals (Hg, Pb, Zn), organic pollutants (PAHs and PCBs), total organic carbon (TOC), total nitrogen (TN), and Holocene paleodepth at the four sampling stations.

appearance of large oyster and horse mussel shells (*Modiolus* sp.) in the upper early and the late TST. In both cores, a major shell bed between 35 and 8 cm depth is primarily formed by large oysters in the lower part and by *Arca noae* shells (still co-occurring with oysters and *Modiolus* sp.) in the upper part. Three dated oysters from this core interval vary in age

between 5,900 and 6,800 years, showing that the shell bed initiated during the MFZ (Tomašových et al. 2019). This stratigraphic pattern indicates that the establishment of biogenic hard bottoms with epifaunal biostromes was initially patchy, and that the shell bed became spatially more continuous ~ 6,500–6,000 years ago. In the Piran 2 core, between 12 and 14 cm, the

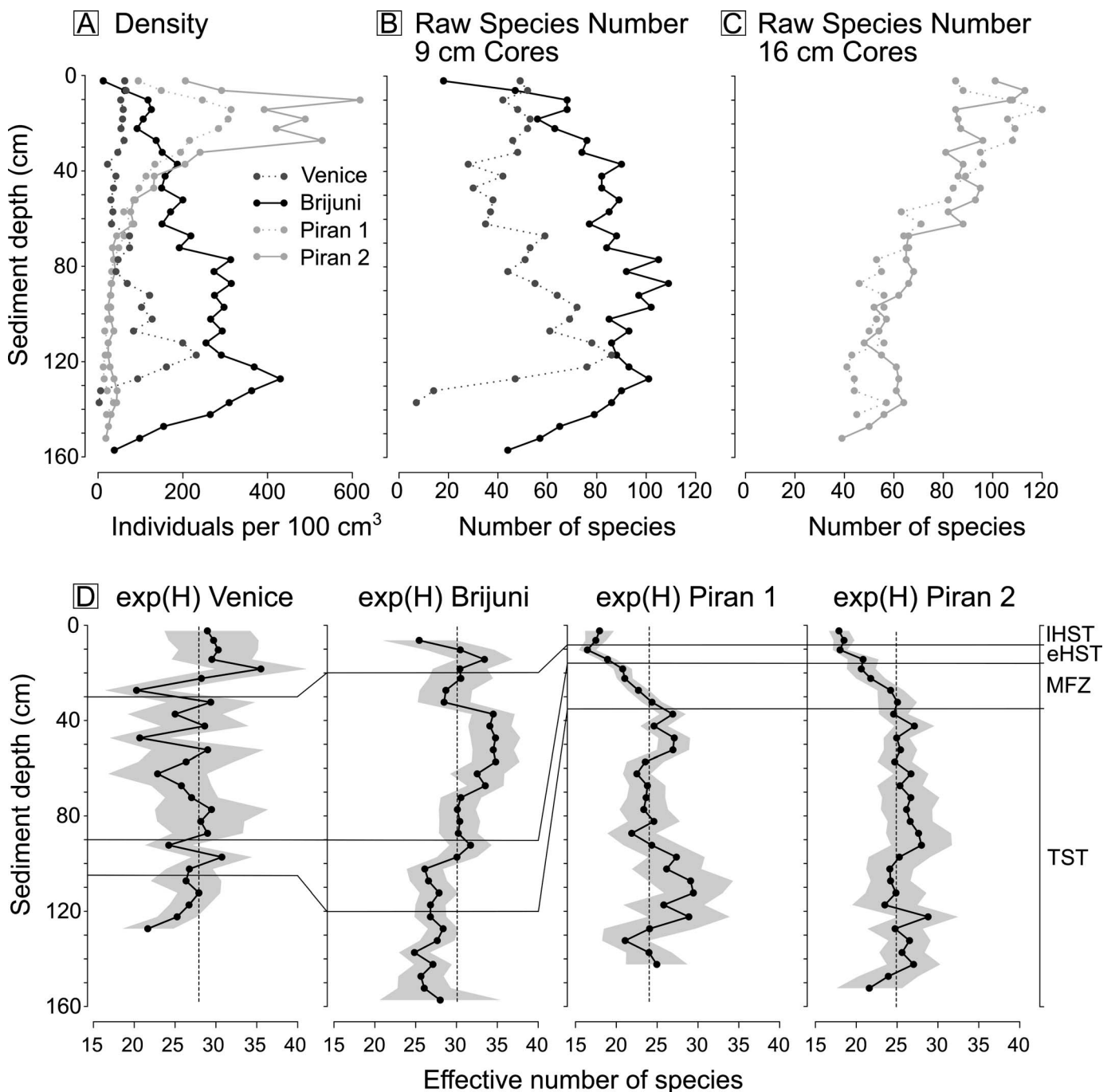


FIG. 11.—Observed trends. **A**) Density. **B**) Raw species numbers for 9-cm-diameter cores. **C**) Raw species numbers for 16-cm-diameter cores. **D**) Diversity, expressed as “effective number of species”, $\exp(H)$, in the mollusk cores from the four sampling stations. Gray shadows of diversity curves represent lower and upper 95% confidence intervals, dotted vertical lines represent the median of each station, and horizontal lines across the graphs mark phase boundaries.

number of fully-grown *Arca* shells is particularly high. Algae-associated grazers such as *Bittium* spp. and several rissoid species considerably increase in abundance within the shell bed. The uppermost 8 cm are clearly separated from the underlying units by (1) a decrease in biogenic gravel; (2) a marked decrease in overall abundance; and (3) a re-establishment of an infauna-dominated soft-bottom community similar to the early TST, with opportunistic species such as *C. gibba* proportionally increasing. On the biocoenosis level, species of the coastal-detritic community are dominant in both cores. However, the transgressive phases are well

separated from the upper core mainly due to a larger proportion of species typical for coastal terrigenous muds and for unstable soft bottoms (Fig. 12B, Online Supplemental File Fig. S6).

Geography Versus Stratigraphy

Variation partitioning based on Hellinger distances shows that a major part of total species and ecological compositional variation observed at the four stations is explained by geographic differentiation (57% with species

TABLE 5.—Differences between stratigraphic units in individual cores with regard to species composition, biocoenosis, feeding guilds, and types of weed-association. The Wilcoxon-rank test was used for the exponential of the Shannon index. For all other comparisons, permutational multivariate analysis of variance (PERMANOVA) was applied, with pseudo-F statistics and probability listed. Significant p-values accounting for multiple tests with the sequential Bonferroni correction at $\alpha = 0.05$ are in bold. For each sampling station, the first four rows list comparisons between consecutive stratigraphic phases; in the following rows phases that do not show significant differences in composition are pooled. Results for the two Piran stations are very similar and are therefore listed only for Piran 1. x = not tested.

	Species composition		Biocoenosis		Feeding guild		Weed association		exp(H)
	F	p-value	F	p-value	F	p-value	F	p-value	p-value
Venice									
IHST2 vs. IHST1	0.88	0.679	0.18	1.000	0.46	0.849	0.51	0.711	x
IHST1 vs. eHST	1.81	0.004	1.96	0.077	2.85	0.026	1.96	0.126	x
eHST vs. MFZ	1.99	0.011	1.50	0.185	2.48	0.035	1.19	0.363	0.945
MFZ vs. TST	2.11	0.017	3.28	0.017	5.46	0.018	6.37	0.019	0.571
IHST vs. eHST	2.13	0.002	2.38	0.026	3.72	0.006	2.49	0.058	0.083
eHST vs. MFZ+TST	5.44	0.001	4.35	0.001	9.35	0.001	6.40	0.002	0.473
HST vs. MFZ + TST	x	x	4.168	0.001	x	x	5.43	0.002	0.198
Brijuni									
IHST vs. eHST2	2.4	0.006	3.44	0.061	2.74	0.064	2.59	0.067	0.352
eHST2 vs. eHST1	4.63	0.001	6.60	0.005	10.82	0.002	9.710	0.004	0.852
eHST1 vs. MFZ	3.99	0.002	13.04	0.001	3.46	0.014	13.040	0.002	0.008
MFZ vs. TST	2.07	0.013	2.95	0.007	4.00	0.018	1.470	0.209	0.345
IHST+eHST2 vs. eHST1	x	x	10.15	0.003	5.08	0.003	6.190	0.003	0.573
eHST1 vs. MFZ+TST	8.30	0.001	x	x	9.17	0.001	22.102	0.001	x
HST vs. MFZ+TST	x	x	x	x	x	x	x	x	< 0.0001
Piran Stations									
IHST vs. eHST	1.45	0.101	2.94	0.064	1.76	0.214	2.33	0.095	1.000
eHST vs. MFZ	2.22	0.013	5.12	0.009	7.61	0.003	5.61	0.014	0.133
MFZ vs. TST1	2.91	0.004	6.23	0.001	6.75	0.001	12.84	0.002	0.067
TST1 vs. TST2	7.05	0.001	15.50	0.001	9.47	0.001	8.56	0.001	0.914
HST vs. MFZ	3.95	0.001	7.46	0.001	16.69	0.001	11.25	0.001	0.029
MFZ vs. TST	x	x	x	x	x	x	x	x	0.026
HST vs. MFZ+TST	x	x	x	x	x	x	x	x	< 0.0001

data, 60% with biocoenoses, 52% with feeding guilds, and 52% with weed-association data), far exceeding the explanatory power of stratigraphic variation at the scale of 5-cm increments (i.e., the explanatory variable is represented by sediment depth; 4% with species data, 5% with biocoenoses, 3% with feeding guilds, and 6% with weed-association data). However, eliminating the geographic component, the contribution of stratigraphic variation to total compositional variation is still higher than under a null hypothesis of no temporal change (F [species] = 12.1, $p < 0.001$, F [biocoenoses] = 12.1, $p < 0.001$, F [feeding guilds] = 12.1, $p < 0.001$, F [weed association] = 17.6, $p < 0.001$).

Differences in grain size between the Venice station and the eastern sites indicate that, at Venice, stronger bottom currents continuously removed finer sediment fractions. Spatial and stratigraphic trends in TOC and TN are probably determined by higher organic content at times of transgression, generating an up-core decline in TOC at all stations except Brijuni, and by differences in mixing, erasing anthropogenic signals in the uppermost core parts at Venice and at Piran 2. Multivariate analyses of species and functional composition point to significant community differences among stations (with the exception of the two Piran stations) and to stratigraphic differences within stations (Table 5).

The largest inter-site distances emerge in the ordination of species composition (Fig. 12A), without any overlaps among the three regions Venice, Brijuni, and Piran, while the cores from the two Piran stations are not separated. The separation of the three regions follows a gradient in grain size (mud-content) and sediment organic content (TOC, TN) responsible for the detached position of the Venice station with its nutrient-poor, sandy sediments on the left side of the NMDS plot. The strongly diverging species composition in the three regions is reflected in the differences among biocoenoses (Fig. 12B), which appear equally

separated in ordination space and further emphasize the heterogeneity of benthic habitats in the northern Adriatic.

The ordination of the four stations according to functional species descriptors (feeding guild and weed-association) leads to a similar, albeit less pronounced compositional separation. The clear separation of Venice with regard to feeding guilds (Fig. 12C) and weed-association is caused by a high proportion of mollusks with chemosymbionts (mainly *L. divaricata*) and of species strictly associated with seagrasses, respectively (Online Supplemental File Figs. S7, S8). Brijuni and Piran stations are functionally more similar and show almost no separation along the first axis (Figs. 12C, 10D). Highstand assemblages at Piran (both Piran stations congruent) and Brijuni overlap in ordination space owing to the abundance of grazers. This group plays an important role throughout the core at Brijuni, while at Piran they emerge as a constitutive feeding guild only between 10 and 30 cm depth (Online Supplemental File Fig. S6). Similar overlaps of intermediate core depths between Brijuni and Piran are also shown for weed-association (Fig. 12D) due to parallel increasing trends in algae-associated species.

The distinction of different stratigraphic units and subunits within the individual cores is more accentuated in the analysis of species composition and biocoenoses than on the functional level, and more pronounced at Brijuni and Piran stations than at Venice (Table 5). At Piran, the eHST and IHST are not significantly different in any ordination but are always distinctly separated from the other units. These units are also clearly distinguished along the first axis, pointing to significant within-core community shifts (Fig. 12). At Brijuni, only the ordination of species composition significantly resolves all major phases. On the functional and biocoenotic level, eHST 2 and IHST form a homogeneous group, as well as TST and MFZ with regard to feeding guilds and weed-association. At Venice, TST and MFZ merge in all ordinations and differ significantly

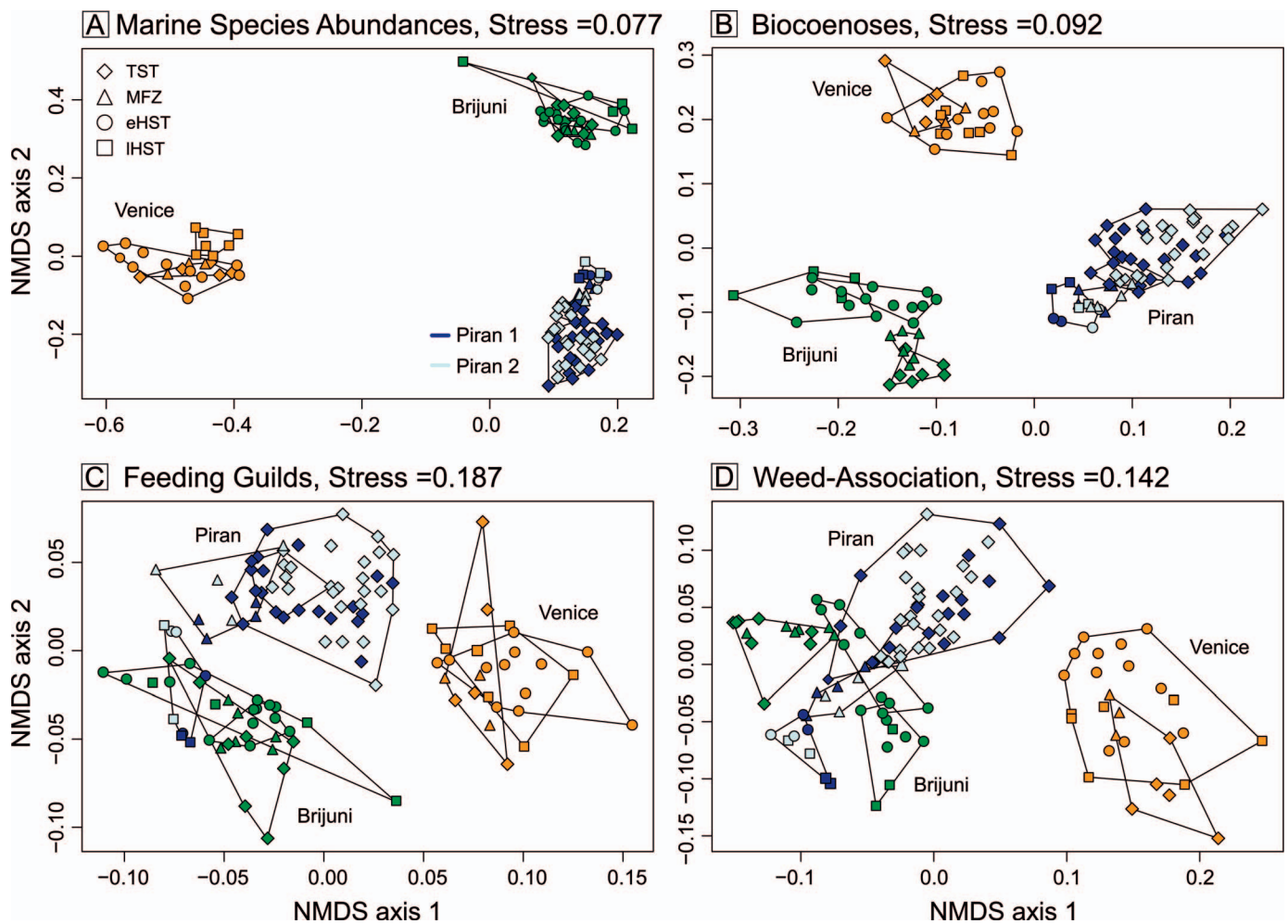


FIG. 12.—Ordinations of the four mollusk cores according to species abundances and three different ecological classifications. **A)** Marine species abundances. **B)** Biocoenotic affiliation. **C)** Feeding guild affiliation. **D)** Type of weed-association. Venice in orange, Brijuni in dark green, Piran 1 in dark blue, and Piran 2 in light blue. The four major phases (transgressive, maximum flooding zone, early, and late highstand) are represented by different symbols; subunits are not graphically distinguished. Hulls delimit significantly different phases and subunits within cores.

from the HST phases due to their high percentage of seagrass-associated species (Table 5).

Environmental Drivers of Community Change

The drivers of up-core mollusk community change identified by forward-selection-model based RDA are either proportions of mud or correlates of pollution and organic enrichment (concentrations of Pb, TN and PCB) that distinguish the uppermost part of the core from the rest. At the two Piran stations, which are characterized by a grain size composition strongly changing up-core, the mud content is the most important variable explaining $\sim 40\%$ of the compositional variation in the dataset (Fig. 13C, 13D). In addition, Pb concentration is selected as a second driver raising the percentage of explained variation to $\sim 48\%$ at Piran 2 (Table 6).

Pb and TN concentrations at Brijuni and concentrations of PCBs at Venice represent the main sources of within-core variation in species composition (Table 6). However, redundancy analyses for each station using only one variable at a time show that several variables are significantly influencing community change (Online Supplemental File Table S9). Many of the elemental concentrations and grain size percentages are strongly correlated (Online Supplemental File Table S10), indicating that the variables picked by forward selection represent two major

environmental vectors: (1) correlates of sedimentary processes affecting sedimentation rate, winnowing and physical reworking (grain size), and (2) correlates of organic enrichment and pollution.

DISCUSSION

Age dating of bivalve shells reveals that at all stations, the sediment cores capture the whole or most of the environmental history since the flooding of the northern Adriatic shelf $\sim 11,000$ years ago (at ~ 40 m water depth, as directly documented at Brijuni; Schnedl et al. 2018) or $\sim 9,000$ years ago (at ~ 20 m water depth) (Antonioli et al. 2007; Storms et al. 2008; Vacchi et al. 2016). In all cores, the major phases of the Holocene marine history (transgressive, maximum flooding zone, early and late highstand phase) can be distinguished on the basis of stratigraphic changes in species and functional composition of mollusk assemblages, as detected by multivariate analyses (Table 5). However, we note that geographic differences overwhelm within-core stratigraphic variation in composition, most likely due to millennial-scale averaging and between-increment mixing that occurs within stratigraphic units (Fig. 7). For example, unmixing of abundance trajectories based on shell ages of two bivalve species showed that a major nineteenth century decline in abundance of *Gouldia minima* and a twentieth century increase in abundance of *Corbula*

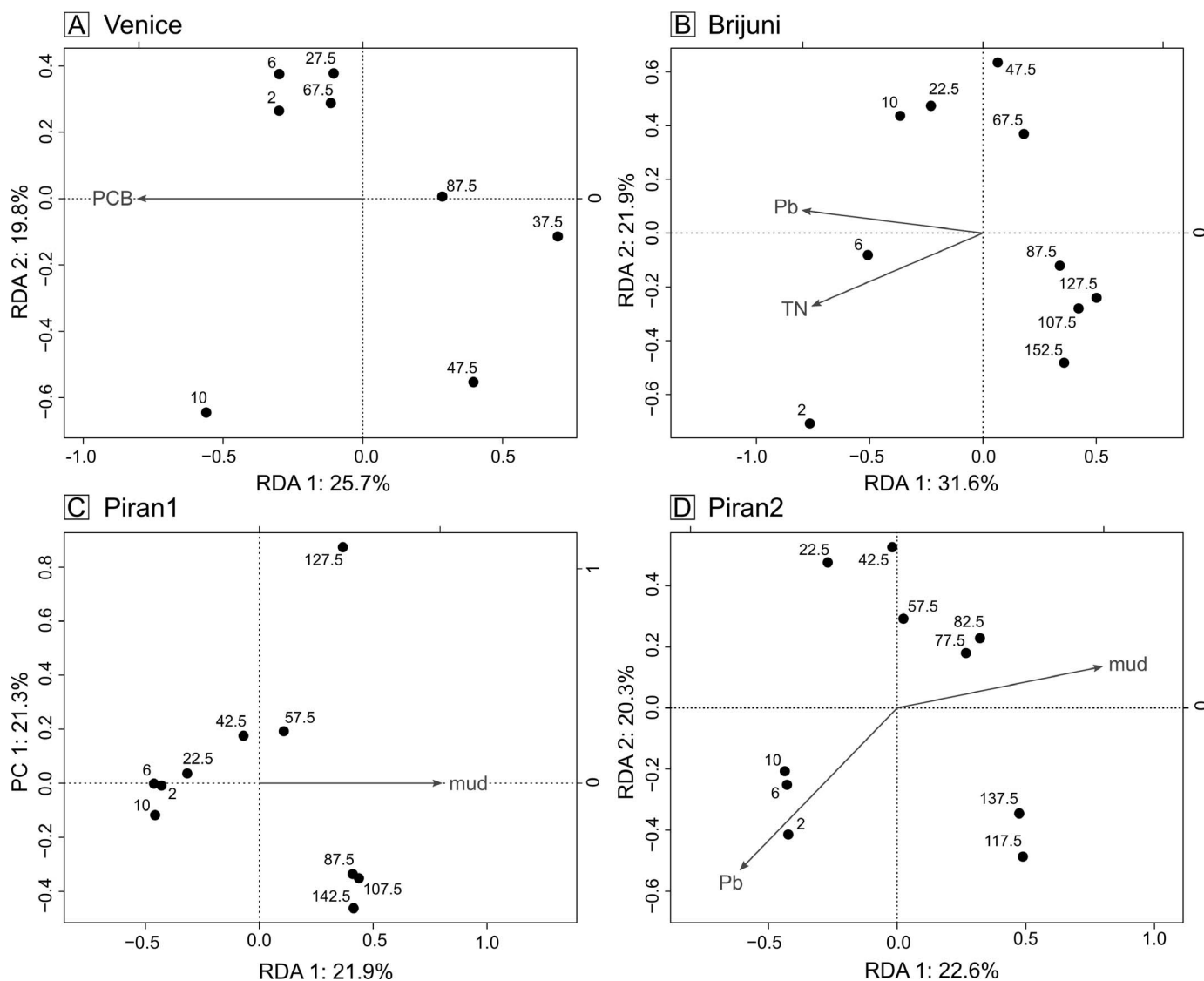


FIG. 13.—RDAs based on the forward selection model for each of the four sampling stations. Additional information (R2 adj., AIC, F- and p-values) is summarized in Table 6. Note that only those core increments that include geochemical data are considered in the RDA.

gibba are significantly muted in the stratigraphic record of highstand units at both Piran stations (Tomašových et al. 2019). The mismatches between ²¹⁰Pb-based apparent sedimentation rates and sedimentation rates based on down-core changes in median shell ages also indicate that the ²¹⁰Pb profiles are steepened by incomplete mixing reaching to 10–20 cm at Brijuni and Piran and to 50 cm at Venice, i.e., below the base of the fully-mixed surface layer (Fig. 3).

The benthic community development in the TST and MFZ follows natural environmental changes such as a deepening of the habitats due to rising sea level and the concomitant establishment of the modern circulation system in the northern Adriatic Sea (Cattaneo and Trincardi 1999), leading to a weakening of the hydrodynamic forces at Brijuni but to intensification of current activity at Piran and at Venice. After sea level stabilization in the eHST, the established communities remained compositionally stable for a few millennia. They can be considered as baseline communities that started to change markedly with the intensification of human impacts on the sea in the IHST. Depending on the sampling region, these baseline communities display specific characteristics.

Establishment and Decline of Seagrass Environments at Venice Station

The lowermost core interval (135–105 cm) encompasses the TST from ~ 10,000 to 6000 years ago and represents a transgressive lag deposit with a mixture of terrestrial and shallow-marine species (Kidwell 1989; Fürsich and Oschmann 1993; Cattaneo and Steel 2003; Scarponi et al. 2017) with the highest mollusk shell abundances in the whole core. Besides the many

TABLE 6.—Statistical parameters of RDA based on the forward selection model.

Station	Variable	R2.adj	AIC	F	p-value
Venice	PCB	0.074	-11.948	1.557	0.024
Brijuni	Pb	0.334	-14.989	5.517	0.002
	TN	0.429	-15.868	2.335	0.014
Piran1	mud	0.405	-20.201	7.138	0.002
Piran2	mud	0.422	-22.079	7.563	0.002
	Pb	0.478	-22.430	1.855	0.018

opercula of the fresh-water snail *Bythinia* sp. evidencing the pre-transgression limnic environments at this site (Amarosi et al. 2008), several species are characteristic for the environmental conditions in the initial phase of marine flooding. The surf clam *Donax venustus* (associated with sandy intertidal and shallow subtidal habitats), and the shallow-water miliolid foraminifer *Massilina* cf. *secans* display the highest abundances in this unit, whereas they are rare in the eHST and completely missing in the IHST. Another shallow-water foraminifer, *Ammonia* cf. *beccarii*, indicating shallow-water marginal environments (Felja et al. 2015) and potentially epiphytic on *Posidonia oceanica* (Debenay et al. 1998), is also abundant. The lucinid bivalve *Lucinella divaricata*, which is commonly associated with seagrass meadows (e.g., Covazzi Harriague et al. 2006), shows highest abundance in the TST, and the two strictly seagrass-associated rissoid bivalves *Rissoa monodonta* and *R. membranacea* (Gofas et al. 2011; Marina et al. 2012) are restricted to this phase. All these taxa contribute to the compositional separation of the lower core section from the upper units (Table 5). They provide evidence for the establishment of seagrass meadows, which probably reached their greatest extent close to the end of the late-Quaternary sea-level rise (Taviani 1980; Correggiari et al. 1996). Dead rhizome mats of *P. oceanica* still occur in a discontinuous belt along the northern Adriatic Italian coast at water depths between 15 and 23 m (Newton and Stefanon 1982; Rismondo et al. 1997). One of the many localities where such remains were found is located very close to the Venice station (Rismondo et al. 1997, fig. 2). Because these rhizome mats have not been dated so far, their age cannot be specified.

The decline and eventual disappearance of seagrasses has been primarily attributed to anthropogenic impacts such as deterioration of water transparency due to eutrophication or increased sediment load (e.g., Taviani 1980; Rismondo et al. 1997). Our findings, however, indicate that seagrasses at this station had already receded during the early HST and were largely eliminated in the late HST. The invertebrate community in the core increasingly features indicator species for barren sandy seafloors affected by strong currents (e.g., *Echinocyamus pusillus* (Telford et al. 1983), *Glycymeris glycymeris* (Royer et al. 2013), and *Paphia rhomboides* (Savina and Pouvreau 2004)). Species with a strict seagrass association are missing in the upper eHST and IHST record.

The decline of seagrasses can be linked to the establishment of the modern circulation pattern in the northern Adriatic after highstand conditions were reached (Trincardi et al. 1994). In the region of the Venice sampling station and generally along a 10–20 m isobath off the Italian coast, strong bottom currents developed, which may have enhanced the erosion of the meadows and increased water turbidity (Stefanon 1984; Casellato and Stefanon 2008). In addition, extreme climatic events such as exceptional storms and diseases could have further contributed to the recession of *P. oceanica* independent of anthropogenic disturbances (Duarte et al. 2006). Therefore, the community at Venice station towards the end of the eHST most likely consisted of an assemblage adapted to sandy seafloor influenced by regular, strong tidal currents and occasional storms, and interspersed with areas covered by meadows of *P. oceanica*.

Brijuni: From Vegetated Habitats and Shell Beds to Bryozoan Meadows

Similar to Venice station, the Brijuni core contains ample evidence for the transition from a terrestrial to a marine environment and for shallow-water habitats in the early TST. The lowest core unit contains high abundances of reworked, poorly preserved terrestrial and freshwater gastropods and a large proportion of organic material originating from the underlying paralic layer. At the time of the marine transgression, the Brijuni station, which today is located a few hundred meters from the coast, was probably close to the rocky slope of the hill now forming the island of Veliki Brijuni. In accord with this, in the deepest core layers, the dominant mollusk species are characteristic of hard bottoms and marine vegetation, partly with a strong but not strict association with seagrasses,

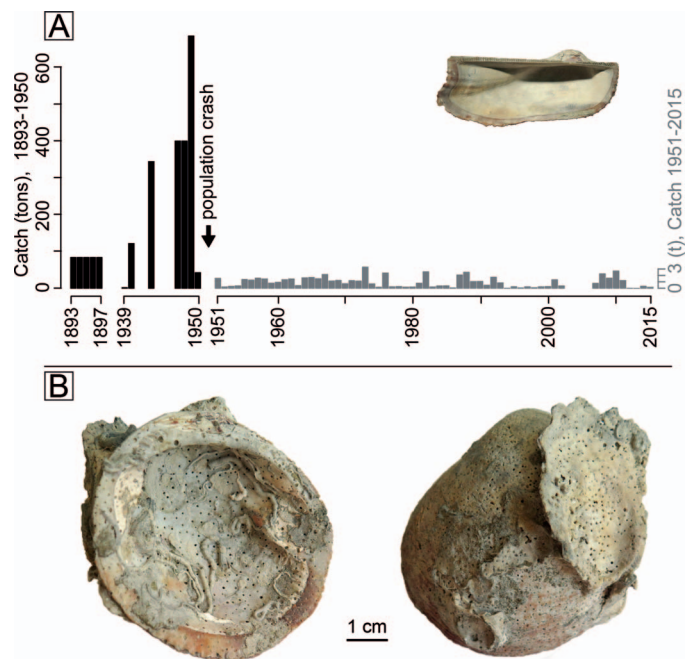


FIG. 14.—**A**) Catch data for *Arca noae* in the northern Adriatic Sea between 1893 and 2015, compiled from the following sources: Krisch (1900): data for 1893–1897; Hrs-Brenko (1980): data for 1940, 1943, and 1947–1949; Biological database of the Fisheries Research Institute of Slovenia (<http://www.biosweb.org/?task=stat#tabs-year>): data for 1939 and 1951–2015. Mind the two different scales in the graph: gray scale outer right for gray bars (1951–2015), black scale outer left for black bars. **B**) *Glycymeris glycymeris* shell from the late TST of the Brijuni core (110–115 cm). Radiocarbon dating of this shell yielded an age of 7,800 years. The type of encrustation indicates the position of the shell on the sediment surface at the time of colonization by epifauna. Left: inner shell surface resting on the sediment, encrusted by serpulids and bryozoans. Right: outer shell surface exposed to the water column, with remains of cemented oyster shells.

thus reflecting a mixed seagrass-hard-bottom habitat in shallow water. As seen at the Venice station, this lowermost core interval features the highest mollusk abundance in the whole core.

With increasing water depth, the mollusk community shifted to a dominance of large-sized bivalve species with epifaunal (scallops, oysters) or shallow-burrowing infaunal life habit (e.g., *Glycymeris glycymeris*, *Timoclea ovata*) and a preference for coarse and detritic bottoms. In the core, this community is preserved in a shell bed containing large and heavily encrusted *Glycymeris* shells (7,800 years old) that provided a settlement basis for arcids and oysters, which are present only in this core unit (Fig. 14B). This shell bed represents the transition from the late transgressive to the earliest highstand phase (MFZ).

As water depth increased and highstand conditions were reached, more fine-grained material was deposited at higher rate leading to increasing siltation of the seafloor. The high percentage of bryozoan gravel at the end of the MFZ (up from 90 cm) indicates a re-organization of the benthic community: faunal elements, particularly the erect bryozoans *Cellaria* sp. (the most abundant bryozoan in the core), *Smittina cervicornis*, and *Myriapora truncata*, dominate while seagrass habitats vanish (40 m of water depth represent the lower range limit of *P. oceanica*; Gobert et al. 2006). This trend is also reflected in the mollusk record where seagrass-associated species decline. *Cellaria* meadows of this kind form a characteristic facies of circalittoral detritic bottoms in the northeastern Adriatic (Seneš 1988a, 1988b; UNEP/MAP-RAC/SPA and Cerrano 2015) and were described as early as 1928 by Vatova (1928). In the vicinity of Rovinj, Croatia, such meadows occur at ~ 35 m depth on detritic bottoms

influenced by currents (McKinney and Jaklin 2000; Novosel 2005). By means of tubular rhizoids, *Cellaria* sp. is able to attach not only on small hard substrates but also directly in the sediment. Thus, it is well adapted to seafloor siltation, to which it can contribute by acting as a sediment trap (McKinney and Jaklin 2001; Hayward and McKinney 2002). While the overall abundance of mollusks decreased during the eHST, their diversity reached a peak, with many epifaunal and several infaunal species. This diverse, bryozoan-dominated benthos, at Brijuni, persisted relatively unchanged into the IHST (uppermost 20 cm).

Development of Arca and Oyster Banks at the Piran Stations

At the Piran stations, water energy increased and sedimentation rate declined through time. The shell bed that was established during the MFZ continued to remain active during the highstand phase. This persistence is in contrast to Brijuni station where oceanographic changes (primarily increasing water depth and resulting sediment siltation and water turbidity) were associated with a decline in water energy and an increase in sedimentation rate, thus driving transgressive to early highstand community shifts that contributed to the loss of shell-beds. At Piran, transgressive sediments have a high proportion of silt, which decreases towards the surface in favor of sand and gravel. The coarser fraction mainly consists of shell fragments whose size increases up-core. With the establishment of the modern circulation system in the northern Adriatic at the end of the TST ~ 7,000–6,000 years ago (Asioli et al. 1996), stronger bottom currents led to an increased winnowing of finer particles, to reduced sedimentation rates and thus to stabilization of the seafloor favoring colonization by epifauna (Mautner et al. 2018). Once established, epifauna-dominated communities were enhanced by positive feedback effects such as (1) the positive dependence of larval survivorship on the abundance of adult conspecifics and (2) taphonomic feedback processes by which dead hard parts of epifauna facilitate the settlement of other epifauna and inhibit burrowing activities of infauna at the same time (Kidwell and Jablonski 1983; Mautner et al. 2018). These developments culminate with the establishment of extensive banks with *Arca* and *Modiolus* between 4,000 and 2,000 years ago. In the cores, this community is represented as a massive shell bed from 35 to 8 cm core depth. Only at Piran 1 station is a similar but less condensed assemblage of large shells of epifaunal mollusks found at the transition between the early and late TST (95–45 cm). These densely colonized and highly diverse *Arca*/oyster bottoms persisted over large areas of the northern Adriatic Sea until the beginning of the twentieth century (Mancini 1929) before human impacts lead to their extirpation.

Human-Induced Degradation of Pre-Anthropogenic Communities

In all cores, signatures of pronounced shifts in the quality of the marine environment and in the benthic communities occur in the uppermost 10–20 cm. These shifts can be directly or indirectly related to human activities. The signatures of shifts are represented by (1) a marked decrease in density and effective species richness at Brijuni and both Piran stations, but not at Venice, and (2) a drop in the effective number of species, except for the Piran 1 station. On the functional level, these changes lead to infauna-dominated communities and in terms of feeding guilds to an increase of suspension feeders at the expense of grazers (Brijuni, Piran) and deposit-feeders (Venice). This convergent and uniform functional trend is all the more remarkable given the strong differences among stations in terms of their sediment composition and water depth.

Venice: Eutrophication and Bottom Trawling.—Human activities contributed in a number of ways to the alteration of the benthic baseline community at the Venice station: (1) Early manipulations of the sedimentation regime of northern Adriatic rivers (e.g., Piave, Adige) by means of river alterations during Roman times and the subsequent collapse

of these structures in the early Middle Ages, which led to enhanced sediment input into the basin and to increased water turbidity—a stressor for the growth of deeper seagrass meadows (Amorosi et al. 2008; Carton et al. 2009; Fontana et al. 2014); (2) Increasing eutrophication of the northern Adriatic Sea during the nineteenth and twentieth centuries negatively impacted seagrass growth not only by reducing water transparency but also by enhancing epiphytic leaf overgrowth and thus hampering photosynthesis (Justić 1988, 1991; Rismondo et al. 1997; Gobert et al. 2006; Gilad et al. 2018); and (3) Intensive bottom trawling, which was practiced in this area as early as in the eighteenth century by the Italian fishing fleets from the city of Chioggia (“chioggioti”), became a decisive factor in the alteration of northern Adriatic soft bottoms after the industrialization of fisheries in the twentieth century and an exponential increase of fishing effort (Krisch 1900; Fortibuoni 2009; Fortibuoni et al. 2010). Pollution seems to play a minor role at this station. Although RDA selects PCBs as a proxy for up-core community change, maximum PCB values remain below Threshold Effects Levels, and PCB co-varies positively with concentrations of nitrogen and carbon, indicating that it correlates with a general eutrophication trend.

Brijuni: Pollution, Eutrophication, Siltation.—The highest pollution values of all four sampling stations including high concentrations of several heavy metals (Hg, Zn, Pb) and organic pollutants (PAHs and PCBs) were observed in the IHST units of the Brijuni core (Fig. 10; see also Schnedl et al. 2018). The most probable sources are the industrial port of Pula located very close to the sampling station, and the use of the Brijuni islands area as a naval port during the late nineteenth and most of the twentieth century (Mlakar 1971; Fabianovic and Matijasec 2008). In addition to elevated contaminant levels, rising concentrations of total nitrogen in the uppermost core increments reflect ongoing eutrophication in this area mainly due to wastewater and agricultural discharge (Howarth 2008). Eutrophication and heavy metal contamination are highlighted in the RDA as the main factors influencing community change in surficial sediments. Furthermore, sediment siltation increases in the uppermost increments in spite of the absence of major sea-level fluctuations and can thus be attributed to human influences. Two factors are likely to contribute to siltation: (1) An increase in soil erosion due to extensive deforestation during the Roman period and in the late Middle Ages (Beug 1977; Oldfield et al. 2003; Kaligarić et al. 2006; Kranjc 2009), and (2) Excavation and construction activities in the nearby harbor of Pula and associated dispersal of sediment plumes by tidal currents. While bottom trawling is a widespread and intensely practiced fishing method in the northern Adriatic Sea, the Brijuni sampling station was protected from this disturbance at least over the last 30 years due to its location within the boundaries of the Brijuni Islands National Park, which was established in 1983 (Fatovic-Ferencic 2006). Nevertheless, the recent community shifts at this station, with rapidly declining density and diversity, a loss of grazers and increase of infaunal species in the uppermost 20 cm, illustrate the strong effects of cumulative human pressures on soft-bottom benthic assemblages and their difficulty in recovering despite decades of protection (Guarnieri et al. 2016).

Piran: Bottom Trawling and Hypoxic Events.—While the concentration of several heavy metals (e.g., Hg and Zn) and of PAHs are high in the IHST unit of the Piran stations and may negatively affect some benthic biota (Mautner et al. 2018), the crucial factors in disrupting the extensive *Arca* beds were most likely the growing pressures from bottom trawling and frequent hypoxic/anoxic events in the twentieth century (Gallmetzer et al. 2017; Tomašových et al. 2017). On fishing maps for the northern Adriatic Sea from the beginning of the twentieth century, wide areas are demarcated where the seafloor was still covered by “banchi di mussoli” (Italian for “*Arca noae* banks”) and which are described as danger zones

for bottom trawlers due to the damage this seafloor cover could cause to fishing gear (Mancini 1929). Both Piran stations fall within this area.

However, with the modernization of fisheries between the two world wars (boats were increasingly equipped with motors, and new, larger and more destructive trawls were employed), the *Arca* beds were soon completely eradicated, and by the 1950s the last *Arca* communities had vanished from northern Adriatic soft bottoms (Fortibuoni 2009; Lotze et al. 2011; Mautner et al. 2018). A compilation of catch data for *Arca noae* in the northern Adriatic illustrates the population crash around 1950 and the dramatic resource exploitation in the preceding years (Fig. 14A). Populations of this species in the Adriatic Sea are characterized by slow growth rate and are thus sensitive to over-exploitation (Peharda et al. 2002; Peharda et al. 2006). Similar scenarios of industrialized mollusk harvesting leading to the destruction of molluscan biostromes (particularly oyster banks) and to a profound alteration of extensive benthic ecosystems appear to have occurred worldwide in the late nineteenth and early twentieth century (e.g., Edgar and Samson 2004; Thurstan et al. 2013).

An additional stressor for the northern Adriatic benthic communities in the second half of the twentieth century are hypoxic or anoxic events whose frequency increased drastically towards the 80s and 90s leading to die-offs of benthic organisms over wide areas (Justić 1991; Stachowitsch 1991; Riedel et al. 2012; Tomašových et al. 2017). Such repeated events keep benthic communities permanently at an early stage of recovery with moderate diversity and dominance by small-sized individuals (Gallmetzer et al. 2017). Meanwhile, infaunal and opportunistic, resistant species such as *C. gibba* are promoted (Occhipinti-Ambrogi et al. 2005; Mavric et al. 2010; Nerlović et al. 2011; Tomašových et al. 2018), while epifauna persists predominantly in the form of isolated, patchy aggregations around fast-growing species (e.g., ascidians and sponges) (Riedel et al. 2012; Tomašových et al. 2017).

CONCLUSIONS

The three locations in the northern Adriatic Sea markedly differ in molluscan community composition and in important habitat-forming environmental drivers, in particular sediment composition and grain size. Because all cores reach back to the marine transgression at the beginning of the Holocene, the sedimentological and geochemical composition of each sediment column epitomizes a site-specific, long-term interaction of multiple shifting environmental factors and ecological feedbacks. These range from shifting bottom current patterns, increasing water depth, changing sediment and nutrient input, to recent anthropogenic disturbances such as pollution and sea-floor perturbation by fishing gear. Our results suggest that habitat differences between sites might have been even more pronounced in earlier phases of the Holocene before human impact peaked in modern times.

In the three sampling areas—Venice, Brijuni, and Piran—different benthic communities established in accord with the prevailing sedimentological and oceanographic conditions. These communities emerged during the eHST (Venice, Brijuni) or the MFZ (Piran) after sea level and circulation had reached their modern character, and persisted over several hundred to thousands of years.

At some sampling stations, in the course of the Holocene, very similar communities became established, persisted for a limited time, and then vanished following diverging environmental developments. For example, during the MFZ, at both the Brijuni and Piran stations, epifaunal communities were established probably due to reduced sedimentation rate coupled with high availability of large dead bivalve shells on the seafloor (preserved in the core as a shell bed). At Piran, these assemblages were at the beginning of a succession leading to the formation of extensive beds with *Arca* and *Modiolus*, which represent the baseline community at this station. At Brijuni, however, different oceanographic conditions and

increasing siltation favored the development of epifaunal assemblages dominated by bryozoans.

The anthropogenic impacts causing decline or downfall of baseline communities are either historical or very recent, depending on the sampling stations. For example, human-induced siltation processes caused by soil erosion due to deforestation and land use (as visible from the Brijuni core) can reach back several millennia, whereas the impact of bottom trawling and hypoxia became crucial only in the twentieth century. Recent and direct impacts such as bottom trawling can quickly alter benthic communities already affected by long-term stressors such as increasing siltation or eutrophication (probably over a few years or decades, as at the Piran stations).

Long-term community changes over the Holocene were primarily driven by gradual changes in sediment composition and/or sea level. Anthropogenic disturbances affected the benthos either by repeated severe impacts (fishing, hypoxic or anoxic events) or gradual changes (eutrophication, pollution). These changes also led to a marked shift of the physical and structural parameters of the substrate, as is the case for bottom trawling. By removing the living cover from the seafloor (e.g., seagrass meadows at Venice station, epifaunal shelly assemblages at Piran), dredging reduces natural filtering capacity and enhances resuspension processes. Thus, benthic communities suffer the double impact of direct damage and of gradual changes of sediment texture and sedimentation regime.

At all stations, regardless of differences in sediment composition and water depth, the human-induced alteration of baseline communities involves a shift towards infauna-dominated communities and a decline of epifaunal forms. The trend is paralleled by an increase of suspension-feeding species at the expense of grazers (Brijuni, Piran) and deposit-feeders (Venice). This profound ecological change reduced species diversity and affected life habits indicating that modern soft-bottom benthic communities in the northern Adriatic Sea no longer show the high geographic variability of the pre-anthropogenic benthos.

ACKNOWLEDGMENTS

Many thanks to the captain of the coring vessel, Jernej Sedmak, for his tireless commitment during the coring campaign in summer 2013. We thank Christa Hermann and Assistant Professor Dr. Robert Peticzka (Laboratory of Physical Geography, University of Vienna) for their help with grain size analysis, and Graham Oliver for his assistance with the identification of bivalves. We thank Thomas Olszewski and two anonymous reviewers for their helpful comments on the manuscript. Adam Tomašových was supported by the Slovak Research and Development Agency (APVV 17-0155) and by the Slovak Scientific Grant Agency (VEGA 0169/19). This work was funded by the Austrian Science Fund (FWF): P24901.

SUPPLEMENTAL MATERIAL

Data are available from the PALAIOS Data Archive: <http://www.sepm.org/pages.aspx?pageid=332>.

REFERENCES

- AIROLDI, L. AND BECK, M.W., 2007, Loss, status and trends for coastal marine habitats of Europe: *Oceanography and Marine Biology: An Annual Review*, v. 45, p. 345–405.
- ALBANO, P.G., GALLMETZER, I., HASELMAIR, A., TOMAŠOVÝCH, A., STACHOWITSCH, M., AND ZUSCHIN, M., 2017, Historical ecology of an alien invasion: the interplay of eutrophication and pollution determines time lags in establishment and detection: *Biological Invasions*, v. 20, p. 1417–1430, doi: 10.1007/s10530-017-1634-7.
- ALBANO, P.G., TOMAŠOVÝCH, A., STACHOWITSCH, M., AND ZUSCHIN, M., 2016, Taxonomic sufficiency in a live-dead agreement study in a tropical setting: *Palaeogeography, Palaeoclimatology, Palaeoecology*, v. 449, p. 341–348, doi: 10.1016/j.palaeo.2016.02.031.
- ALLEN, A.P., KOSNIK, M.A., AND KAUFMAN, D.S., 2013, Characterizing the dynamics of amino acid racemization using time-dependent reaction kinetics: a Bayesian approach to fitting age-calibration models: *Quaternary Geochronology*, v. 18, p. 63–77, doi: 10.1016/j.quageo.2013.06.003.

- AMOROSI, A., BRUNO, L., CAMPO, B., MORELLI, A., ROSSI, V., SCARPONI, D., HONG, W., BOHACS, K.M., AND DREXLER, T.M., 2017, Global sea-level control on local parasequence architecture from the Holocene record of the Po Plain, Italy: *Marine and Petroleum Geology*, v. 87, p. 99–111, doi: 10.1016/j.marpetgeo.2017.01.020.
- AMOROSI, A., DINELLI, E., ROSSI, V., VAIANI, S.C., AND SACCHETTO, M., 2008, Late Quaternary palaeoenvironmental evolution of the Adriatic coastal plain and the onset of Po River Delta: *Palaeogeography, Palaeoclimatology, Palaeoecology*, v. 268, p. 80–90, doi: 10.1016/j.palaeo.2008.07.009.
- AMOROSI, A., FONTANA, A., ANTONIOLI, F., PRIMON, S., AND BONDESAN, A., 2008, Post-LGM sedimentation and Holocene shoreline evolution in the NW Adriatic coastal area: *Geoacta*, v. 7, p. 41–67.
- ANDERSON, L.C., MCBRIDE, R.A., TAYLOR, M.J., AND BYRNES, M.R., 1998, Late Holocene record of community replacement preserved in time-averaged molluscan assemblages, Louisiana Chenier Plain: *PALAIOS*, v. 13, p. 488–499, doi: 10.2307/3515476.
- ANDERSON, M.J., 2001, A new method for non-parametric multivariate analysis of variance: *Austral Ecology*, v. 26, p. 32–46, doi: 10.1111/j.1442-9993.2001.01070.pp.x.
- ANTONIOLI, F., ANZIDEI, M., LAMBECK, K., AURIEMMA, R., GADDI, D., FURLANI, S., ORRÙ, P., SOLINAS, E., GASPARI, A., KARINJA, S., KOVAČIĆ, V., AND SURACE, L., 2007, Sea-level change during the Holocene in Sardinia and in the northeastern Adriatic (central Mediterranean Sea) from archaeological and geomorphological data: *Quaternary Science Reviews*, v. 26, p. 2463–2486, doi: 10.1016/j.quascirev.2007.06.022.
- ASIOLI, A., TRINCARDI, F., CORREGGIARI, A., LANGONE, L., VIGLIOTTI, L., VAN DER KAARS, S., AND LOWE, J., 1996, The Late-Quaternary Deglaciation in the Central Adriatic Basin: II Quaternario Italian Journal of Quaternary Sciences, v. 9, p. 763–770.
- BARMAWIDJAJA, D.M., VAN DER ZWAAN, G.J., JORISSEN, F.J., AND PUSCARIC, S., 1995, 150 years of eutrophication in the northern Adriatic Sea: evidence from a benthic foraminiferal record: *Marine Geology*, v. 122, p. 367–384.
- BEUG, H.-J., 1977, Vegetationsgeschichtliche Untersuchungen im Küstenbereich von Istrien (Jugoslawien): *Flora*, v. 166, p. 357–381, doi: 10.1016/s0367-2530(17)32153-9.
- BRAMBATI, A., 1992, Origin and evolution of the Adriatic Sea, in G. Colombo, I. Ferrari, U.V. Ceccherelli, and R. Rossi (eds.), *Marine Eutrophication and Population Dynamics: Olson and Olson, Fredensborg, Denmark*, p. 327–346.
- BRÖCKER, W., MATSUMOTO, K., CLARK, E., HAJDAS, I., AND BONANI, G., 1999, Radiocarbon age differences between coexisting foraminiferal species: *Paleoceanography*, v. 14, p. 431–436, doi: 10.1029/1999PA000019.
- CARTON, A., BONDESAN, A., FONTANA, A., MENEGHEL, M., MIOLA, A., MOZZI, P., PRIMON, S., AND SURIAN, N., 2009, Geomorphological evolution and sediment transfer in the Piave River system (northeastern Italy) since the Last Glacial Maximum: *Géomorphologie: Relief, Processus, Environnement*, v. 15, p. 155–174.
- CASEBOLT, S. AND KOWALEWSKI, M., 2018, Mollusk shell assemblages as archives of spatial structuring of benthic communities around subtropical islands: *Estuarine, Coastal and Shelf Science*, v. 215, p. 132–143, doi: 10.1016/j.ecss.2018.09.023.
- CASELLATO, S. AND STEFANON, A., 2008, Coralligenous habitat in the northern Adriatic Sea: an overview: *Marine Ecology*, v. 29, p. 321–341, doi: 10.1111/j.1439-0485.2008.00236.x.
- CATTANEO, A. AND STEEL, R.J., 2003, Transgressive deposits: a review of their variability: *Earth-Science Reviews*, v. 62, p. 187–228.
- CATTANEO, A. AND TRINCARDI, F., 1999, The late Quaternary transgressive record in the Adriatic Epicontinental Sea: basin widening and facies partitioning, in K.M. Bergman and J.W. Snedden (eds.), *Isolated Shallow Marine Sand Bodies: Sequence Stratigraphic Analysis and Sedimentologic Interpretation: SEPM Society for Sedimentary Geology Special Publication 64*, p. 127–146.
- CATUNEANU, O., ABREU, V., BHATTACHARYA, J.P., BLUM, M.D., DALRYMPLE, R.W., ERIKSSON, P.G., FIELDING, C.R., FISHER, W.L., GALLOWAY, W.E., GIBLING, M.R., GILES, K.A., HOLBROOK, J.M., JORDAN, R., KENDALL, C.G.S.C., MACURDA, B., MARTINSEN, O.J., MIALL, A.D., NEAL, J.E., NUMMEDAL, D., POMAR, L., POSAMANTIER, H.W., PRATT, B.R., SARG, J.F., SHANLEY, K.W., STEEL, R.J., STRASSER, A., TUCKER, M.E., AND WINKER, C., 2009, Towards the standardization of sequence stratigraphy: *Earth-Science Reviews*, v. 92, p. 1–33, doi: 10.1016/j.earscirev.2008.10.003.
- CHAO, A., GOTELLI NICHOLAS, J., HSIEH, T.C., SANDER ELIZABETH, L., MA, K.H., COLWELL ROBERT, K., AND ELLISON AARON, M., 2014, Rarefaction and extrapolation with Hill numbers: a framework for sampling and estimation in species diversity studies: *Ecological Monographs*, v. 84, p. 45–67, doi: 10.1890/13-0133.1.
- CLARKE, K.R. AND WARWICK, R.M., 2001, Change in marine communities: an approach to statistical analysis and interpretation, second edition: PRIMER-E Ltd, Plymouth, 175 p.
- COLANTONI, P., GALLIGNANI, P., AND LENAZ, R., 1979, Late Pleistocene and Holocene evolution of the North Adriatic continental shelf (Italy): *Marine Geology*, v. 33, p. M41–M50, doi: 10.1016/0025-3227(79)90130-0.
- COLANTONI, P. AND MENCUCCHI, D., 2010, Some remarks on sediment dispersion in the Central-western Adriatic continental shelf: *Geoacta, Special Publication 3*, p. 57–87.
- COLL, M. AND LOTZE, H.K., 2016, Ecological Indicators and Food-Web Models as Tools to Study Historical Changes in Marine Ecosystems, in K. Schwerdtner Mäñez and B. Poulsen (eds.), *Perspectives on Oceans Past, A Handbook of Marine Environmental History: Springer, Dordrecht*, p. 103–132.
- COLL, M., PIRODDI, C., ALBOUY, C., BEN RAIS LASRAM, F., CHEUNG, W.W.L., CHRISTENSEN, V., KARPOUZI, V.S., GUILHAUMON, F., MOULLOT, D., PALECZNY, M., PALOMARES, M.L., STEENBEEK, J., TRUJILLO, P., WATSON, R., AND PAULY, D., 2012, The Mediterranean Sea under siege: spatial overlap between marine biodiversity, cumulative threats and marine reserves: *Global Ecology and Biogeography*, v. 21, p. 465–480, doi: 10.1111/j.1466-8238.2011.00697.x.
- CORREGGIARI, A., FIELD, M.E., AND TRINCARDI, F., 1996, Late Quaternary transgressive large dunes on the sediment-starved Adriatic shelf, in M. De Batist and P. Jacobs (eds.), *Geology of Siliciclastic Shelf Seas: Geological Society, London, Special Publication 117*, p. 155–169.
- COVAZZI HARRIAGUE, A., BIANCHI, C.N., AND ALBERTELLI, G., 2006, Soft-bottom macrobenthic community composition and biomass in a *Posidonia oceanica* meadow in the Ligurian Sea (NW Mediterranean): *Estuarine, Coastal and Shelf Science*, v. 70, p. 251–258, doi: 10.1016/j.ecss.2005.10.017.
- CRAMER, K.L., LEONARD-PINGEL, J.S., RODRÍGUEZ, F., AND JACKSON, J.B.C., 2015, Molluscan subfossil assemblages reveal the long-term deterioration of coral reef environments in Caribbean Panama: *Marine Pollution Bulletin*, v. 96, p. 176–187, doi: 10.1016/j.marpolbul.2015.05.031.
- DEBENAY, J.-P., BÉNÉTEAU, E., ZHANG, J., STOUFF, V., GESLIN, E., REDOIS, F., AND FERNANDEZ-GONZALEZ, M., 1998, *Ammonia beccarii* and *Ammonia tepida* (Foraminifera): morphofunctional arguments for their distinction: *Marine Micropaleontology*, v. 34, p. 235–244, doi: 10.1016/S0377-8398(98)00010-3.
- DIAKOVAC, T., DEGOBBIS, D., SUPIĆ, N., AND PRECALI, R., 2012, Marked reduction of eutrophication pressure in the northeastern Adriatic in the period 2000–2009: *Estuarine, Coastal and Shelf Science*, v. 115, p. 25–32, doi: 10.1016/j.ecss.2012.03.029.
- DOMINGUEZ, J.G., KOSNIK, M.A., ALLEN, A.P., HUA, Q., JACOB, D.E., KAUFMAN, D.S., AND WHITACRE, K., 2016, Time-averaging and stratigraphic resolution in death assemblages and Holocene deposits: sydney harbour's molluscan record: *PALAIOS*, v. 31, p. 564–575, doi: 10.2110/palo.2015.087.
- DUARTE, C.M., FOURQUREAN, J.W., KRAUSE-JENSEN, D., AND OLESEN, B., 2006, Dynamics of seagrass stability and change, in A. Larkum, R. Orth, and C. Duarte (eds.), *Seagrasses: Biology, Ecology and Conservation: Springer, The Netherlands, Dordrecht*, p. 271–294.
- EDGAR, G.J. AND SAMSON, C.R., 2004, Catastrophic decline in mollusc diversity in eastern Tasmania and Its Concurrence with Shellfish Fisheries: *Conservation Biology*, v. 18, p. 1579–1588, doi: 10.1111/j.1523-1739.2004.00191.x.
- FATOVIC-FERENCIC, S., 2006, Brijuni Archipelago: story of Kuppelwieser, Koch, and Cultivation of 14 Islands: *Croatian Media Journal*, v. 47, p. 369–371.
- FELIA, I., FONTANA, A., FURLANI, S., BAJRAKTAJEVIĆ, Z., PARADZIK, A., TOPALOVIC, E., ROSSATO, S., COSOVIC, V., AND JURACIĆ, M., 2015, Environmental changes in the lower Mirna River valley (Istria, Croatia) during the middle and late Holocene: *Geologia Croatica*, v. 68, p. 209–224.
- FERRETTI, F., OSIO, G.C., JENKINS, C.J., ROSENBERG, A.A., AND LOTZE, H.K., 2013, Long-term change in a meso-predator community in response to prolonged and heterogeneous human impact, v. 3, p. 1057, doi: 10.1038/srep01057, <https://www.nature.com/articles/srep01057#supplementary-information>.
- FIORINI, F. AND VAIANI, S.C., 2001, Benthic foraminifers and transgressive-regressive cycles in the late Quaternary subsurface sediments of the Po Plain near Ravenna (Northern Italy): *Bollettino della Società Paleontologica Italiana*, v. 40, p. 357–403.
- FONTANA, A., MOZZI, P., AND MARCHETTI, M., 2014, Alluvial fans and megafans along the southern side of the Alps: *Sedimentary Geology*, v. 301, p. 150–171, doi: 10.1016/j.sedgeo.2013.09.003.
- FORTIBUONI, T., 2009, La pesca in Alto Adriatico dalla caduta della Serenissima ad oggi: un'analisi storica ed ecologica: Ph.D. Thesis, Università degli studi di Trieste, Trieste, 258 p.
- FORTIBUONI, T., LIBRALATO, S., RAICEVICH, S., GIOVANARDI, O., AND SOLIDORO, C., 2010, Coding early naturalists' accounts into long-term fish community changes in the Adriatic Sea (1800–2000): *PLoS ONE*, v. 5, p. e15502, doi: 10.1371/journal.pone.0015502.
- FRIGNANI, M., LANGONE, L., RAVAIOLI, M., SORGENTE, D., ALVISI, F., AND ALBERTAZZI, S., 2005, Fine-sediment mass balance in the western Adriatic continental shelf over a century time scale: *Marine Geology*, v. 222–223, p. 113–133.
- FÜRSICH, F.T. AND OSCHMANN, W., 1993, Shell beds as tools in basin analysis: the Jurassic of Kachhh, western India: *Journal of the Geological Society*, v. 150, p. 169–185, doi: 10.1144/gsjgs.150.1.0169.
- GALLMETZER, I., HASELMAIR, A., STACHOWITSCH, M., AND ZUSCHIN, M., 2016, An innovative piston corer for large-volume sediment samples: *Limnology and Oceanography: Methods*, v. 14, p. 698–717, doi: 10.1002/lom3.10124.
- GALLMETZER, I., HASELMAIR, A., TOMAŠOVÝCH, A., STACHOWITSCH, M., AND ZUSCHIN, M., 2017, Responses of molluscan communities to centuries of human impact in the northern Adriatic Sea: *PLoS ONE*, v. 12, p. e0180820, doi: 10.1371/journal.pone.0180820.
- GIANI, M., DIAKOVAC, T., DEGOBBIS, D., COZZI, S., SOLIDORO, C., AND UMANI, S.F., 2012, Recent changes in the marine ecosystems of the northern Adriatic Sea: *Estuarine, Coastal and Shelf Science*, v. 115, p. 1–13, doi: 10.1016/j.ecss.2012.08.023.
- GILAD, E., KIDWELL, S.M., BENAYAHU, Y., AND EDELMAN-FURSTENBERG, Y., 2018, Unrecognized loss of seagrass communities based on molluscan death assemblages: historic baseline shift in tropical Gulf of Aqaba, Red Sea: *Marine Ecology Progress Series*, v. 589, p. 73–83.
- GOBERT, S., CAMBRIDGE, M.L., VELIMIROV, B., PERGENT, G., LEPOINT, G., BOUQUEGNEAU, J.-M., DAUBY, P., PERGENT-MARTINI, C., AND WALKER, D.I., 2006, Biology of *Posidonia*, in A.W.D. Larkum, R.J. Orth, and C.M. Duarte (eds.), *Seagrasses: Biology, Ecology and Conservation: Springer, Dordrecht, The Netherlands*, p. 387–408.
- GOÑAS, S., MORENO, D., AND SALAS, C., 2011, Moluscos Marinos de Andalucía: Servicio de Publicaciones e Intercambio Científico, Universidad de Málaga, Málaga, 798 p.

- GOSLAR, T., CZERNIK, J., AND GOSLAR, E., 2004, Low-energy ^{14}C AMS in Poznań Radiocarbon Laboratory, Poland: Nuclear Instruments and Methods in Physics Research Section B: Beam Interactions with Materials and Atoms, v. 223-224, p. 5–11, doi: 10.1016/j.nimb.2004.04.005.
- GUARNIERI, G., BEVILACQUA, S., DE LEO, F., FARELLA, G., MAFFIA, A., TERLIZZI, A., AND FRASCHETTI, S., 2016, The challenge of planning conservation strategies in threatened seascapes: understanding the role of fine scale assessments of community response to cumulative human pressures: PLoS ONE, v. 11, p. e0149253, doi: 10.1371/journal.pone.0149253.
- HAYWARD, P.J. AND MCKINNEY, F.K., 2002, Northern Adriatic Bryozoa from the vicinity of Rovinj, Croatia: Bulletin of the American Museum of Natural History, v. 270, p. 139.
- HRS-BRENKO, M., 1980, Preliminary survey of populations of the bivalve Noah's ark (*Arca noae*, Linné) in the northern Adriatic Sea: Aquaculture, v. 21, p. 357–363.
- HSIEH, T.C., MA, K.H., AND CHAO, A., 2016, iNEXT: an R package for rarefaction and extrapolation of species diversity (Hill numbers). Methods in Ecology and Evolution, v. 7, p. 1451–1456.
- HOWARTH, R.W., 2008, Coastal nitrogen pollution: A review of sources and trends globally and regionally: Harmful Algae, v. 8, p. 14–20.
- HUNT, D. AND TUCKER, M.E., 1992, Stranded parasequences and the forced regressive wedge systems tract: deposition during base-level fall: Sedimentary Geology, v. 81, p. 1–9, doi: 10.1016/0037-0738(92)90052-S.
- JACKSON, J.B.C., KIRBY, M.X., BERGER, W.H., BJORNDA, K.A., BOTSFORD, L.W., BOURQUE, B.J., BRADBURY, R.H., COOKE, R., ERLANDSON, J., ESTES, J.A., HUGHES, T.P., KIDWELL, S., LANGE, C.B., LENIHAN, H.S., PANDOLFI, J.M., PETERSON, C.H., STENECK, R.S., TEGNER, M.J., AND WARNER, R.R., 2001, Historical overfishing and the recent collapse of coastal ecosystems: Science, v. 293, p. 629–637.
- JOST, L., 2007, Partitioning diversity into independent alpha and beta components: Ecology, v. 88, p. 2427–2439, doi: 10.1890/06-1736.1.
- JUSTIĆ, D., 1988, Trend in the transparency of the Northern Adriatic Sea 1911–1982: Marine Pollution Bulletin, v. 19, p. 32–35.
- JUSTIĆ, D., 1991, Hypoxic conditions in the northern Adriatic Sea: historical development and ecological significance, in R.V. Tyson and T.H. Pearson (eds.), Modern and Ancient Continental Shelf Anoxia: Geological Society of London, Special Publication 58, p. 95–105.
- KALIGARIC, M., CULIBERG, M., AND KRAMBERGER, B., 2006, Recent vegetation history of the North Adriatic Grasslands: expansion and decay of an anthropogenic habitat: Folia Geobotanica, v. 41, p. 241–258.
- KAUFMAN, D.S. AND MANLEY, W.F., 1998, A new procedure for determining DL amino acid ratios in fossils using reverse phase liquid chromatography: Quaternary Science Reviews, v. 17, p. 987–1000, doi: 10.1016/S0277-3791(97)00086-3.
- KIDWELL, S., 1989, Stratigraphic condensation of marine transgressive records; origin of major shell deposits in the Miocene of Maryland: Journal of Geology, v. 97, p. 1–24.
- KIDWELL, S.M., 2002, Time-averaged molluscan death assemblages: palimpsests of richness, snapshots of abundance: Geology, v. 30, p. 803–806, doi: 10.1130/0091-7613(2002)030<0803:tamdap>2.0.co;2.
- KIDWELL, S.M., 2015, Biology in the Anthropocene: challenges and insights from young fossil records: Proceedings of the National Academy of Sciences, v. 112, p. 4922–4929, doi: 10.1073/pnas.1403660112.
- KIDWELL, S. AND JABLONSKI, D., 1983, Taphonomic feedback ecological consequences of shell accumulation, in M. Tevesz and P. McCall (eds.), Biotic Interactions in Recent and Fossil Benthic Communities: Springer, Boston, MA, p. 195–248.
- KOSNIK, M., HUA, Q., KAUFMAN, D., AND ZAWADZKI, A., 2015, Sediment accumulation, stratigraphic order, and the extent of time-averaging in lagoonal sediments: a comparison of ^{210}Pb and ^{14}C /amino acid racemization chronologies: Coral Reefs, v. 34, p. 215–229, doi: 10.1007/s00338-014-1234-2.
- KOSNIK, M.A., HUA, Q., JACOBSEN, G.E., KAUFMAN, D.S., AND WUST, R.A., 2007, Sediment mixing and stratigraphic disorder revealed by the age-structure of *Tellina* shells in Great Barrier Reef sediment: Geology, v. 35, p. 811–814.
- KOSNIK, M.A. AND KAUFMAN, D.S., 2008, Identifying outliers and assessing the accuracy of amino acid racemization measurements for geochronology: II, data screening: Quaternary Geochronology, v. 3, p. 328–341.
- KOWALEWSKI, M., CASEBOLT, S., HUA, Q., WHITACRE, K.E., KAUFMAN, D.S., AND KOSNIK, M.A., 2018, One fossil record, multiple time resolutions: disparate time-averaging of echinoids and mollusks on a Holocene carbonate platform: Geology, v. 46, p. 51–54, doi: 10.1130/G39789.1.
- KOWALEWSKI, M., WITTMER, J.M., DEXTER, T.A., AMOROSI, A., AND SCARPONI, D., 2015, Differential responses of marine communities to natural and anthropogenic changes: Proceedings of the Royal Society B, v. 282, doi: 10.1098/rspb.2014.2990.
- KRANJC, A., 2009, History of Deforestation and Reforestation in the Dinaric karst: Geographical Research, v. 47, p. 15–23, doi: 10.1111/j.1745-5871.2008.00552.x.
- KRISCH, A., 1900, Fischerei im Adriatischen Meere mit besonderer Berücksichtigung der österreichisch-ungarischen Küsten: Carl Gerold's Sohn in Wien, Pola, 280 p.
- LEGENDRE, P. AND DE CÁCERES, M., 2013, Beta diversity as the variance of community data: dissimilarity coefficients and partitioning: Ecology Letters, v. 16, p. 951–963, doi: 10.1111/ele.12141.
- LEGENDRE, P. AND GALLAGHER, E.D., 2001, Ecologically meaningful transformations for ordination of species data: Oecologia, v. 129, p. 271–280, doi: 10.1007/s004420100716.
- LONG, E.R., MACDONALD, D.D., SMITH, S.L., AND CALDER, F.D., 1995, Incidence of adverse biological effects within ranges of chemical concentrations in marine and estuarine sediments: Journal of Environmental Management, v. 19, p. 81–97.
- LOTZE, H.K., COLL, M., AND DUNNE, J.A., 2011, Historical changes in marine resources, food-web structure and ecosystem functioning in the Adriatic Sea, Mediterranean: Ecosystems, v. 14, p. 198–222, doi: 10.1007/s10021-010-9404-8.
- LOTZE, H.K., LENIHAN, H.S., BOURQUE, B.J., BRADBURY, R.H., COOKE, R.G., KAY, M.C., KIDWELL, S.M., KIRBY, M.X., PETERSON, C.H., AND JACKSON, J.B.C., 2006, Depletion, degradation, and recovery potential of estuaries and coastal seas: Science, v. 312, p. 1806–1809.
- MANCINI, L., 1929, Crociere di pesca per lo studio del fondo marino, Golfo di Trieste e costa occidentale istriana, anno 1927: Ministero dell' Economia Nazionale, Direzione Generale dell' Industria e delle Miniere, Genova, 52 p.
- MARINA, P., URRÁ, J., RUEDA, J.L., AND SALAS, C., 2012, Composition and structure of the molluscan assemblage associated with a *Cymodocea nodosa* bed in south-eastern Spain: seasonal and diel variation: Helgolander Marine Research, v. 66, p. 585–599, doi: 10.1007/s10152-012-0294-3.
- MARTINELLI, J.C., SOTO LUIS, P., GONZÁLEZ, J., AND RIVADENEIRA, M., 2017, Benthic communities under anthropogenic pressure show resilience across the Quaternary: Royal Society Open Science, v. 4, p. 170796, doi: 10.1098/rsos.170796.
- MAUTNER, A.-K., GALLMETZER, I., HASELMAIR, A., SCHNEDL, S.-M., TOMAŠOVÝCH, A., AND ZUSCHIN, M., 2018, Holocene ecosystem shifts and human-induced loss of *Arca* and *Ostrea* shell beds in the north-eastern Adriatic Sea: Marine Pollution Bulletin, v. 126, p. 19–30, doi: 10.1016/j.marpolbul.2017.10.084.
- MAVRIC, B., ORLANDO-BONACA, M., BETTOSO, N., AND LIPEJ, L., 2010, Soft-bottom macrozoobenthos of the southern part of the Gulf of Trieste: faunistic, bioecologic and ecological survey: Acta Adriatica, v. 51, p. 203–216.
- MCKINNEY, F.K., 2007, The Northern Adriatic ecosystem: deep time in a shallow sea: Columbia University Press, New York, 328 p.
- MCKINNEY, F.K. AND JAKLIN, A., 2000, Spatial niche partitioning in the *Cellaria* meadow epibiont association, northern Adriatic Sea: Cahiers de Biologie Marine, v. 41, p. 1–17.
- MCKINNEY, F.K. AND JAKLIN, A., 2001, Sediment accumulation in a shallow-water meadow carpeted by a small erect bryozoan: Sedimentary Geology, v. 145, p. 397–410, doi: 10.1016/S0037-0738(01)00156-7.
- MLAKAR, Š., 2017, Brioni: Uprava Brionskih otoka, Pula, 58 p.
- MOZETIČ, P., SOLIDORO, C., COSSARINI, G., SOCAL, G., PRECALI, R., FRANCÉ, J., BIANCHI, F., DE VITTOR, C., SMODLAKA, N., AND FONDA UMANI, S., 2010, Recent trends towards oligotrophication of the Northern Adriatic: evidence from chlorophyll a time series: Estuaries and Coasts, v. 33, p. 362–375, doi: 10.1007/s12237-009-9191-7.
- NERLOVIĆ, V., DOĞAN, A., AND HRS-BRENKO, M., 2011, Response to oxygen deficiency (depletion): bivalve assemblages as an indicator of ecosystem instability in the northern Adriatic Sea: Biologia, v. 66, p. 1114–1126, doi: 10.2478/s11756-011-0121-3.
- NEWTON, R.S. AND STEFANON, A., 1982, Side-scan sonar and subbottom profiling in the northern Adriatic Sea: Marine Geology, v. 46, p. 279–306, doi: 10.1016/0025-3227(82)90085-8.
- NOVOSEL, M., 2005, Bryozoans of the Adriatic Sea: Denisia, v. 16, p. 231–246.
- OCCHIPINTI-AMBROGI, A., 2007, Global change and marine communities: alien species and climate change: Marine Pollution Bulletin, v. 55, p. 342–352, doi: 10.1016/j.marpolbul.2006.11.014.
- OCCHIPINTI-AMBROGI, A., SAVINI, D., AND FORNI, G., 2005, Macrobenthos community structural changes off Cesenatico coast (Emilia Romagna, Northern Adriatic), a six-year monitoring programme: Science of the Total Environment, v. 353, p. 317–328.
- OKSANEN, J., BLANCHET, G., KINDT, R., LEGENDRE, P., MINCHIN, P.R., O'HARA, R.B., SIMPSON, G., SOLYMO, P., HENRY, M., STEVENS, H., AND WAGNER, H., 2016, vegan: Community Ecology Package: R package version 2.3-5, <http://cran.r-project.org/package=vegan>. Checked January 2019.
- OLDFIELD, F., ASIOLI, A., ACCORSI, C.A., MERCURI, A.M., JUGGINS, S., LANGONE, L., ROLPH, T., TRINCARDI, F., WOLFF, G., GIBBS, Z., VIGLIOTTI, L., FRIGNANI, M., VAN DER POST, K., AND BRANCH, N., 2003, A high resolution late Holocene palaeo environmental record from the central Adriatic Sea: Quaternary Science Reviews, v. 22, p. 319–342, doi: 10.1016/S0277-3791(02)00088-4.
- OLSGARD, F. AND SOMERFIELD, P.J., 2000, Surrogates in marine benthic investigations— which taxonomic unit to target?: Journal of Aquatic Ecosystem Stress and Recovery, v. 7, p. 25–42, doi: 10.1023/A:1009967313147.
- PALINKAS, C.M., AND NITTROUER, C.A., 2007, Modern sediment accumulation on the Po shelf, Adriatic Sea: Continental Shelf Research, v. 27, p. 489–505.
- PEHARDA, M., MLADINEO, I., BOLOTIN, J.A., KEKEZ, L., AND SKARAMUCA, B.K., 2006, The reproductive cycle and potential protandric development of the Noah's Ark shell, *Arca noae* L.: implications for aquaculture: Aquaculture, v. 252, p. 317–327, doi: 10.1016/j.aquaculture.2005.07.007.
- PEHARDA, M., RICHARDSON, C.A., ONOFRI, V., BRATOŠ, A., AND CRNČEVIĆ, M., 2002, Age and growth of the bivalve *Arca noae* L. in the Croatian Adriatic Sea: Journal of Molluscan Studies, v. 68, p. 307–310.
- PENG, T.H., BROECKER, W.S., AND BERGER, W.H., 1979, Rates of benthic mixing in deep-sea sediment as determined by radioactive tracers: Quaternary Research, v. 11, p. 141–149, doi: 10.1016/0033-5894(79)90074-7.
- PERES-NETO, P.R., LEGENDRE, P., DRAY, S., AND BORCARD, D., 2006, Variation partitioning of species data matrices: estimation and comparison of fractions: Ecology, v. 87, p. 2614–2625, doi: 10.1890/0012-9658(2006)87[2614:VPOSDM]2.0.CO;2.

- PICONE, S., ALVISI, F., DINELLI, E., MORIGI, C., NEGRI, A., RAVAIOLI, M., AND VACCARO, C., 2008, New insights on late Quaternary palaeogeographic setting in the Northern Adriatic Sea (Italy): *Journal of Quaternary Science*, v. 23, p. 489–501, doi: 10.1002/jqs.1152.
- POIRIER, C., SAURIAL, P.-G., CHAUMILLON, E., AND ALLARD, J., 2009, Can molluscan assemblages give insights into Holocene environmental changes other than sea level rise? A case study from a macrotidal bay (Marennes–Oléron, France): *Palaeogeography, Palaeoclimatology, Palaeoecology*, v. 280, p. 105–118, doi: 10.1016/j.palaeo.2009.06.002.
- R CORE TEAM, 2013, R: A language and environment for statistical computing: R Foundation for Statistical Computing, Vienna, Austria, <http://www.R-project.org/>. Checked January 2019.
- RABALAIS, N.N., DIAZ, R.J., LEVIN, L.A., TURNER, R.E., GILBERT, D., AND ZHANG, J., 2010, Dynamics and distribution of natural and human-caused hypoxia: *Biogeosciences*, v. 7, p. 585–619, doi: 10.5194/bg-7-585-2010.
- REIMER, P.J., BARD, E., BAYLISS, A., BECK, J.W., BLACKWELL, P.G., BRONK RAMSEY, C., BUCK, C.E., CHENG, H., EDWARDS, R.L., FRIEDRICH, M., GROOTES, P.M., GUILDERSON, T.P., HAFLLIDASON, H., HAJDAS, I., HATTÉ, C., HEATON, T.J., HOFFMANN, D.L., HOGG, A.G., HUGHEN, K.A., KAISER, K.F., KROMER, B., MANNING, S.W., NIU, M., REIMER, R.W., RICHARDS, D.A., SCOTT, E.M., SOUTHON, J.R., STAFF, R.A., TURNEY, C.S.M., AND VAN DER PLICHT, J., 2013, IntCal13 and Marine13 Radiocarbon Age Calibration Curves 0–50,000 Years cal BP: *Radiocarbon*, v. 55, p. 1869–1887.
- RIEDEL, B., ZUSCHIN, M., AND STACHOWITSCH, M., 2012, Tolerance of benthic macrofauna to hypoxia and anoxia in shallow coastal seas: a realistic scenario: *Marine Ecology Progress Series*, v. 458, p. 39–52.
- RISMONDO, A., GUIDETTI, P., AND CUIEL, D., 1997, Presenza delle fanerogame marine nel Golfo di Venezia: un aggiornamento: *Bollettino del Museo Civico di Storia Naturale di Venezia*, v. 47, p. 317–328.
- RITTER, M.D.N., ERTHAL, F., KOSNIK, M.A., COIMBRA, J.C., AND KAUFMAN, D.S., 2017, spatial variation in the temporal resolution of subtropical shallow-water molluscan death assemblage: *PALAIOS*, v. 32, p. 572–583, doi: 10.2110/palo.2017.003.
- ROBERTS, C., 2007, *The Unnatural History of the Sea*: Island Press, Washington, DC, USA, 456 p.
- ROSSI, V. AND VAJANI, S.C., 2008, Benthic foraminiferal evidence of sediment supply changes and fluvial drainage reorganization in Holocene deposits of the Po Delta, Italy: *Marine Micropaleontology*, v. 69, p. 106–118, doi: 10.1016/j.marmicro.2008.07.001.
- ROYER, C., THÉBAULT, J., CHAUVAUD, L., AND OLIVIER, F., 2013, Structural analysis and paleoenvironmental potential of dog cockle shells (*Glycymeris glycymeris*) in Brittany, northwest France: *Palaeogeography, Palaeoclimatology, Palaeoecology*, v. 373, p. 123–132, doi: 10.1016/j.palaeo.2012.01.033.
- SANCHEZ-CABEZA, J.A., AND RUIZ-FERNÁNDEZ, A.C., 2012, ²¹⁰Pb sediment radiochronology: an integrated formulation and classification of dating models: *Geochimica et Cosmochimica Acta*, v. 82, p. 183–200, doi: 10.1016/j.gca.2010.12.024.
- SANGIORGI, F. AND DONDEERS, T.H., 2004, Reconstructing 150 years of eutrophication in the north-western Adriatic Sea (Italy) using dinoflagellate cysts, pollen and spores: *Estuarine, Coastal and Shelf Science*, v. 60, p. 69–79, doi: 10.1016/j.ecss.2003.12.001.
- SAVINA, M. AND POUVREAU, S., 2004, A comparative ecophysiological study of two infaunal filter-feeding bivalves: *Paphia rhomboïdes* and *Glycymeris glycymeris*: *Aquaculture*, v. 239, p. 289–306, doi: 10.1016/j.aquaculture.2004.05.029.
- SCARPONI, D., AZZARONE, M., KUSNERIK, K., AMOROSI, A., BOHACS, K.M., DREXLER, T.M., AND KOWALEWSKI, M., 2017, Systematic vertical and lateral changes in quality and time resolution of the macrofossil record: insights from Holocene transgressive deposits, Po coastal plain, Italy: *Marine and Petroleum Geology*, v. 87, p. 128–136, doi: 10.1016/j.marpetgeo.2017.03.031.
- SCARPONI, D., KAUFMAN, D., AMOROSI, A., AND KOWALEWSKI, M., 2013, Sequence stratigraphy and the resolution of the fossil record: *Geology*, v. 41, p. 239–242, doi: 10.1130/g33849.1.
- SCARPONI, D. AND KOWALEWSKI, M., 2007, Sequence stratigraphic anatomy of diversity patterns: Late Quaternary benthic mollusks of the Po plain, Italy: *PALAIOS*, v. 22, p. 296–305.
- SCHNEIDL, S.-M., HASELMAIR, A., GALLMETZER, I., MAUTNER, A.-K., TOMASOVYCH, A., AND ZUSCHIN, M., 2018, Benthic communities at Brižuni Islands (northern Adriatic Sea) were shaped by Holocene sea-level rise and recent human impact: *The Holocene*, v. 28, p. 1801–1817, doi: 10.1177/0959683618788651.
- SENEŠ, J., 1988a, Quantitative analysis of north and south Adriatic shelf ecosystems: *Geologica Carpathica*, v. 39, p. 675–712.
- SENEŠ, J., 1988b, The Island Banjole - a type region of recent marine ecosystems on North Adriatic Shelf: *Geologica Carpathica*, v. 39, p. 713–738.
- SIANI, G., PATERNE, M., ARNOLD, M., BARD, E., MATIVIER, B., TISNERAT, N., AND BASSINOT, F., 2000, Radiocarbon reservoir ages in the Mediterranean Sea and Black Sea: *Radiocarbon*, v. 42, p. 271–280.
- SMODLAKA, N., 1986, Primary production of the organic matter as an indicator of the eutrophication in the northern Adriatic sea: *Science of the Total Environment*, v. 56, p. 211–220, doi: 10.1016/0048-9697(86)90325-6.
- STACHOWITSCH, M., 1991, Anoxia in the Northern Adriatic Sea: rapid death, slow recovery, in R.V. Tyson and T.H. Pearson (eds.), *Modern and Ancient Continental Shelf Anoxia*: Geological Society of London Special Publication 58, p. 119–129.
- STEFANON, A., 1984, Sedimentologia del mare Adriatico: rapporti tra erosione e sedimentazione olocenica: *Bollettino di Oceanologia Teorica ed Applicata*, v. 2, p. 281–324.
- STORMS, J.E.A., WELTJE, G.J., TERRA, G.J., CATTANEO, A., AND TRINCARDI, F., 2008, Coastal dynamics under conditions of rapid sea-level rise: late Pleistocene to early Holocene evolution of barrier-lagoon systems on the northern Adriatic shelf (Italy): *Quaternary Science Reviews*, v. 27, p. 1107–1123, doi: 10.1016/j.quascirev.2008.02.009.
- STUIVER, M. AND POLACH, H.A., 2016, Discussion reporting of ¹⁴C data: *Radiocarbon*, v. 19, p. 355–363, doi: 10.1017/S003822200003672.
- STUIVER, M. AND REIMER, P.J., 2006, Extended (super 14) C data base and revised CALIB 3.0 ¹⁴C age calibration program: *Radiocarbon*, v. 35, p. 215–230.
- TAVIANI, M., 1980, I molluschi dei terreni superficiali della piattaforma continentale alto Adriatico fra la foce del fiume Reno e la laguna veneta, in P. Colantoni and P. Gallignani (eds.), *Ricerche sulla piattaforma continentale dell'alto Adriatico*, Risultati della crociera 1978 (dalla foce del Reno a Venezia): CNR, Bologna, p. 65–80.
- TELFORD, M., HAROLD, A.S., AND MOOI, R., 1983, Feeding structures, behavior, and microhabitat of *Echinocyamus pusillus* (Echinoidea: Clypeasteroidea): *The Biological Bulletin*, v. 165, p. 745–757, doi: 10.2307/1541476.
- TESI, T., MISEROCCHI, S., GOŃI, M.A., TURCHETTO, M., LANGONE, L., DE LAZZARI, A., ALBERTAZZI, S., AND CORREGGIARI, A., 2011, Influence of distributary channels on sediment and organic matter supply in event-dominated coastal margins: the Po prodelta as a study case: *Biogeosciences*, v. 8, p. 365–385, doi: 10.5194/bg-8-365-2011.
- THURSTAN, R.H., HAWKINS, J.P., RABY, L., AND ROBERTS, C.M., 2013, Oyster (*Ostrea edulis*) extirpation and ecosystem transformation in the Firth of Forth, Scotland: *Journal for Nature Conservation*, v. 21, p. 253–261, doi: 10.1016/j.jnc.2013.01.004.
- TOMASOVYCH, A., GALLMETZER, I., HASELMAIR, A., KAUFMAN, D.S., KRALI, M., CASSIN, D., ZONTA, R., AND ZUSCHIN, M., 2018, Tracing the effects of eutrophication on molluscan communities in sediment cores: outbreaks of an opportunistic species coincide with reduced bioturbation and high frequency of hypoxia in the Adriatic Sea: *Paleobiology*, v. 44, p. 575–602, doi: 10.1017/pab.2018.22.
- TOMASOVYCH, A., GALLMETZER, I., HASELMAIR, A., KAUFMAN, D., MAVRIČ, B., AND ZUSCHIN, M., 2019, A decline in molluscan carbonate production driven by the loss of vegetated habitats encoded in the Holocene sedimentary record of the Gulf of Trieste: *Sedimentology*, doi: 10.1111/sed.12516.
- TOMASOVYCH, A., GALLMETZER, I., HASELMAIR, A., KAUFMAN, D.S., VIDOVIĆ, J., AND ZUSCHIN, M., 2017, Stratigraphic unmixing reveals repeated hypoxia events over the past 500 years in the northern Adriatic Sea: *Geology*, v. 45, p. 363–366.
- TOMASOVYCH, A. AND KIDWELL, S.M., 2010, Predicting the effects of increasing temporal scale on species composition, diversity, and rank-abundance distributions: *Paleobiology*, v. 36, p. 672–695, doi: 10.1666/08092.1.
- TOMASOVYCH, A., KIDWELL, S.M., BARBER, R.F., AND KAUFMAN, D.S., 2014, Long-term accumulation of carbonate shells reflects a 100-fold drop in loss rate: *Geology*, v. 42, p. 819–822, doi: 10.1130/G35694.1.
- TOMASOVYCH, A. AND KIDWELL, S.M., 2017, Nineteenth-century collapse of a benthic marine ecosystem on the open continental shelf: *Proceedings of the Royal Society B: Biological Sciences*, v. 284, p. 20170328, doi: 10.1098/rspb.2017.0328.
- TRINCARDI, F., ARGNANI, A., AND CORREGGIARI, A., 2011, Note illustrative della Carta Geologica dei Mari Italiani alla scala 1:250.000, foglio NL 33-7 VENEZIA: ISPRA Servizio Geologico D'Italia, Firenze.
- TRINCARDI, F., CORREGGIARI, A., AND ROVERI, M., 1994, Late Quaternary transgressive erosion and deposition in a modern epicontinental shelf: the Adriatic Semi-enclosed Basin: *Geo-Marine Letters*, v. 14, p. 41–51.
- TROBEC, A., BUSETTI, M., ZGUR, F., BARADELLO, L., BABICH, A., COVA, A., GORDINI, E., ROMEO, R., TOMINI, I., POGLAJEN, S., DIVIACCO, P., AND VRABEC, M., 2018, Thickness of marine Holocene sediment in the Gulf of Trieste (northern Adriatic Sea): *Earth System Science Data*, v. 10, p. 1077–1092, doi: 10.5194/essd-10-1077-2018.
- TURNEY, C.S.M. AND BROWN, H., 2007, Catastrophic early Holocene sea level rise, human migration and the Neolithic transition in Europe: *Quaternary Science Reviews*, v. 26, p. 2036–2041.
- TYLER, C.L. AND KOWALEWSKI, M., 2017, Surrogate taxa and fossils as reliable proxies of spatial biodiversity patterns in marine benthic communities: *Proceedings. Biological sciences*, v. 284, p. 20162839, doi: 10.1098/rspb.2016.2839.
- UNEP/MAP-RAC/SPA, 2015, *Adriatic Sea: Description of the ecology and identification of the areas that may deserve to be protected*: Report by C. Cerrano, edited by D. Cebrian and S. Requena, RAC/SPA, Tunis, 92 p.
- VACCHI, M., MARRINER, N., MORHANGE, C., SPADA, G., FONTANA, A., AND ROVERE, A., 2016, Multiproxy assessment of Holocene relative sea-level changes in the western Mediterranean: sea-level variability and improvements in the definition of the isostatic signal: *Earth-Science Reviews*, v. 155, p. 172–197, doi: 10.1016/j.earscirev.2016.02.002.
- VATOVA, A., 1928, *Compendio della Flora e Fauna del Mare Adriatico* presso Rovigno con la distribuzione geografica delle specie bentoniche: Comitato Talassografico Italiano, Istituto di Biologia Marina per l'Adriatico-Rovigno, Venezia, 614 p.
- VIDOVIĆ, J., NAWROT, R., GALLMETZER, I., HASELMAIR, A., TOMASOVYCH, A., STACHOWITSCH, M., ČOSOVIĆ, V., AND ZUSCHIN, M., 2016, Anthropogenically induced environmental changes in the northeastern Adriatic Sea in the last 500 years (Panzano Bay, Gulf of Trieste): *Biogeosciences*, v. 13, p. 5965–5981, doi: 10.5194/bg-13-5965-2016.
- WARD, T.J. AND HUTCHINGS, P.A., 1996, Effects of trace metals on infaunal species composition in polluted intertidal and subtidal marine sediments near a lead smelter, Spencer Gulf, South Australia: *Marine Ecology Progress Series*, v. 135, p. 123–135.

- ZAVATARELLI, M., RAICICH, F., BREGANT, D., RUSSO, A., AND ARTEGIANI, A., 1998, Climatological biogeochemical characteristics of the Adriatic Sea: *Journal of Marine Systems*, v. 18, p. 227–263.
- ZECCHIN, M., GORDINI, E., AND RAMELLA, R., 2015, Recognition of a drowned delta in the northern Adriatic Sea, Italy: stratigraphic characteristics and its significance in the frame of the early Holocene sea-level rise: *The Holocene*, v. 25, p. 1027–1038, doi: 10.1177/0959683615575358.
- ZILLÉN, L., CONLEY, D.J., ANDRÉN, T., ANDRÉN, E., AND BJÖRCK, S., 2008, Past occurrences of hypoxia in the Baltic Sea and the role of climate variability, environmental change and human impact: *Earth-Science Reviews*, v. 91, p. 77–92, doi: 10.1016/j.earscirev.2008.10.001.
- ZUSCHIN, M. AND STACHOWITSCH, M., 2009, Epifauna-dominated benthic shelf assemblages: lessons from the modern Adriatic Sea: *PALAIOS*, v. 24, p. 211–221, doi: 10.2110/palo.2008.p08-062r.

Received 23 July 2018; accepted 11 January 2019.